ON THE SECOND-ORDER ACCURACY OF VOLUME-OF-FLUID INTERFACE RECONSTRUCTION ALGORITHMS: CONVERGENCE IN THE MAX NORM

ELBRIDGE GERRY PUCKETT

ON THE SECOND-ORDER ACCURACY OF VOLUME-OF-FLUID INTERFACE RECONSTRUCTION ALGORITHMS: CONVERGENCE IN THE MAX NORM

ELBRIDGE GERRY PUCKETT

Given a two times differentiable curve in the plane, I prove that — using only the volume fractions associated with the curve — one can construct a piecewise linear approximation that is second-order in the max norm. I derive two parameters that depend only on the grid size and the curvature of the curve, respectively. When the maximum curvature in the 3 by 3 block of cells centered on a cell through which the curve passes is less than the first parameter, the approximation in that cell will be second-order. Conversely, if the grid size in this block is greater than the second parameter, the approximation in the center cell can be less than second-order. Thus, this parameter provides an a priori test for when the interface is *under-resolved*, so that when the interface reconstruction method is coupled to an adaptive mesh refinement algorithm, this parameter may be used to determine when to *locally* increase the resolution of the grid.

1. Introduction

In this article I study the *interface reconstruction problem* for a volume-of-fluid method in two space dimensions. Let $\Omega \in R^2$ denote a simply connected domain and let $\mathbf{z}(s) = (x(s), y(s))$, where s is arc length, denote a curve in Ω. The *interface reconstruction problem* is to compute an approximation $\tilde{\mathbf{z}}(s)$ to $\mathbf{z}(s)$ in Ω using only the volume fractions due to $\mathbf{z}$ on the grid. I define volume fractions and discuss this problem in more detail in Section 1.1 below.

Let L be a characteristic length of the problem. Cover Ω with a grid consisting of square cells each of side $\Delta x \leq L$ and let

$$h = \frac{\Delta x}{L} \tag{1}$$

be a *dimensionless* parameter that represents the size of a grid cell as a nondimensional quantity. Note that h is bounded above by 1. This ensures that second-order accurate methods, which have $O(h^2)$ error, will be more accurate than first-order accurate methods, which have $O(h)$ error. For the remainder of this article it will be understood that quantities such as the arc length s and the radius of curvature R are also nondimensional quantities obtained by division by L as in (1) and that the curvature κ has been nondimensionalized by dividing by $1/L$.

In this article I prove that a piecewise linear volume-of-fluid interface reconstruction method will be a second-order accurate approximation to the exact interface $\mathbf{z}(s) = (x(s), y(s))$ *in the max norm* provided the following four conditions hold:

I. The interface $\mathbf{z}$ is two times continuously differentiable: $\mathbf{z}(s) \in C^2(\Omega)$.

II. The maximum value

$$\kappa_{\max} = \max_s |\kappa(s)| \tag{2}$$

of the curvature $\kappa(s)$ of $\mathbf{z}(s)$ satisfies[1]

$$\kappa_{\max} \le C_\kappa \equiv \min\{C_h\, h^{-1}, \left(\sqrt{h}\right)^{-1}\}, \tag{3}$$

where C_h is a constant that is independent of h and is defined by

$$C_h \equiv \frac{\sqrt{2} - 1}{4\sqrt{3}}. \tag{4}$$

III. In each cell C_{ij} that contains a portion of the interface, the slope m_{ij} of the piecewise linear approximation

$$\tilde{g}_{ij}(x) = m_{ij}\, x + b_{ij} \tag{5}$$

to the interface in that cell is given by

$$m_{ij} = \frac{S_{i+\alpha} - S_{i+\beta}}{\alpha - \beta} \qquad \text{for } \alpha, \beta = 1, 0, -1 \text{ with } \alpha \ne \beta, \tag{6}$$

where $S_{i+\alpha}$ and $S_{i+\beta}$ denote two distinct *column sums* of volume fractions from the 3×3 block of cells B_{ij} surrounding the cell C_{ij}.[2] The column sums S_{i-1}, S_i, and S_{i+1} are defined and described in more detail in Section 1.3.

IV. The column sums $S_{i+\alpha}$ and $S_{i+\beta}$ in (6) are sufficiently accurate that the slope m_{ij} defined in (6) is a first-order accurate approximation to $g'(x_c)$, where x_c is the center of the bottom edge of the cell C_{ij}.

---

[1]It is only necessary that the maximum curvature of the interface satisfy this condition in a neighborhood of the cell C_{ij} in which one wishes to reconstruct the interface. For example, in the 3×3 block of cells B_{ij} centered on C_{ij}.

[2]I will usually omit the subscript i, j when writing the piecewise linear approximation $\tilde{g}$ defined in (5) and simply write $\tilde{g}(x)$ instead of $\tilde{g}_{ij}(x)$. Similarly, when no confusion is likely to arise, I will drop the subscript i, j from the slope m and the y-intercept b and simply write $\tilde{g}(x) = m\, x + b$.

Section 3 is devoted to proving that if condition (3) above is satisfied, one can always find an orientation of the 3×3 block of cells (say, after rotating by a multiple of 90 degrees) so that there are two column sums $S_{i+\alpha}$ and $S_{i+\beta}$, *both in the same orientation of the 3×3 block*, satisfying the condition in item IV above. Note that here I do not provide an algorithm for determining which orientation of the 3×3 block of cells is the correct one to use or, given a correct orientation, how to find the two column sums to use in (6). What I do prove is that if the interface satisfies Equation (3), then one can find an orientation of the 3×3 block of cells that has two distinct column sums $S_{i+\alpha}$ and $S_{i+\beta}$ such that the slope m_{ij} obtained in (6) is a first-order accurate approximation to $g'(x_c)$ and hence, $\tilde{g}$ is a second-order accurate approximation to g in the max norm as illustrated in Figure 1.[3]
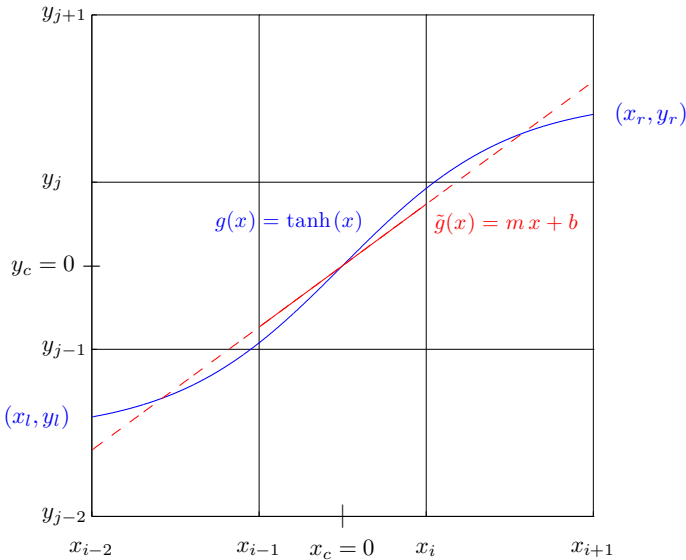
Figure 1. In this example the interface is $g(x) = \tanh x$. All three column sums are exact (in the sense of Section 1.3), but for the inverse function $x = g^{-1}(y)$ only the center column sum is exact. Also plotted is the linear approximation $\tilde{g}(x) = mx + b$ in the center cell produced by the volume-of-fluid interface reconstruction algorithm when the slope m is chosen as half the difference between the first and third column sums. The main result of this paper is that $|g(x) - \tilde{g}(x)| \le Ch^2$ for all $x \in [x_{i-1}, x_i]$ provided that the slope m is defined in the manner described in Section 1.3.

---

[3]In this particular example all three of the column sums S_{i-1}, S_i and S_{i+1} are exact. Consequently, Theorem 23 in Section 4 implies any two of them can be used in (6) and that the resulting slope $m = \tilde{g}'(x_c)$ is a first-order accurate approximation to $g'(x_c)$, regardless of whether one chooses the slope to be $m = (S_i - S_{i-1})$, $m = (S_{i+1} - S_{i-1})/2$, or $m = (S_{i+1} - S_i)$.

A variety of algorithms have been proposed for determining the correct column sums to use to determine the approximate slope via Equation (6). I refer the interested reader to [6; 7; 11; 14; 22; 23; 25; 37] for further information.

Finally, I would like to emphasize that the criteria in (3) provides an a priori test to determine when a given computation of the interface is *well-resolved*; namely, the computation is well-resolved whenever

$$h \leq H_{\max} = \min\{C_h \, (\kappa_{\max})^{-1}, (\kappa_{\max})^{-2}\}. \tag{7}$$

This will enable researchers who employ block structured adaptive mesh refinement to model the motion of an interface [30; 31; 33; 34] to compute an approximation to the curvature of the interface in each cell and then check to see if the conditions in (7) are satisfied in order to determine if the computation is under-resolved in that cell. Cells in which $h > H_{\max}$ are then tagged for refinement. In this regard I note that Sussman and Ohta [32] have developed second- and fourth-order accurate volume-of-fluid algorithms for computing the curvature from the volume fraction information.

1.1. *A detailed statement of the problem.*

Suppose that I am given a simply connected computational domain $\Omega \in R^2$ that is divided into two distinct regions Ω_d and Ω_l so that $\Omega = \Omega_d \cup \Omega_l$. I will refer to Ω_d as the "dark" fluid[4] and to Ω_l as the "light" fluid. Let $\mathbf{z}(s) = (x(s), y(s))$, where s is arc length, denote the *interface* between these two fluids. Cover Ω with a uniform square grid of cells, each with side h, and let Λ_{ij} denote the fraction of dark fluid in the (i, j)-th cell. Each number Λ_{ij} satisfies $0 \leq \Lambda_{ij} \leq 1$ and is called the *volume fraction* (of dark fluid) in the (i, j)-th cell.[5] Note that

$$0 < \Lambda_{ij} < 1 \tag{8}$$

if and only if a portion of the interface $\mathbf{z}(s)$ lies in the (i, j)-th cell and that $\Lambda_{ij} = 1$ (resp. $\Lambda_{ij} = 0$) if the i, j cell only contains dark (resp. light) fluid.

In this paper I consider the following problem. Given only the collection of volume fractions Λ_{ij} in the grid covering Ω I wish to *reconstruct* $\mathbf{z}(s)$; that is, to find a piecewise linear approximation $\tilde{\mathbf{z}}$ to $\mathbf{z}$. Furthermore, the approximate interface $\tilde{\mathbf{z}}$ must have the property that the volume fractions $\tilde{\Lambda}_{ij}$ due to $\tilde{\mathbf{z}}$ are identical to the

---

[4]Although these algorithms have historically been known as "volume-of-fluid" methods, they are frequently used to model the interface between any two materials, including gases, liquids, solids and any combination thereof [8; 16; 17; 18]. However, when analyzing the method, the convention is to refer to the two materials as fluids.

[5]Even though in two dimensions Λ_{ij} is technically an area fraction, the convention is to refer to it as a *volume* fraction.

original volume fractions Λ_{ij}; that is,

$$\tilde{\Lambda}_{ij} = \Lambda_{ij} \quad \text{for all cells } C_{ij}. \tag{9}$$

An algorithm for finding such an approximation is known as a *volume-of-fluid interface reconstruction method*. The property that $\tilde{\Lambda}_{ij} = \Lambda_{ij}$ is the principal feature that distinguishes volume-of-fluid interface reconstruction methods from other interface reconstruction methods. It ensures that the computational value of the total volume of each fluid is exact. In other words, all volume-of-fluid interface reconstruction methods are conservative in that they conserve the volume of each material in the computation. When the underlying numerical method is a conservative finite difference method this can be essential since, for example, in order to obtain the correct shock speed it is necessary for all of the conserved quantities to be conserved by the underlying numerical method; for example, see [5; 17; 18; 26]. More generally, a necessary condition for the numerical method to converge to the correct weak solution of the underlying partial differential equation (PDE) is that all of the quantities that are conserved in the PDE must be conserved by the numerical method [15].

Volume-of-fluid methods have been used by researchers to track material interfaces since at least the early 1970s (see [20; 21], for example), and a variety of such algorithms have been developed for modeling everything from flame propagation [3] to curvature and solidification [4]. In particular, the problem of developing high-order accurate volume-of-fluid methods for modeling the curvature and surface tension of an interface has received much attention [1; 2; 4; 10; 13; 24]. Volume-of-fluid methods were among the first interface tracking algorithms to be implemented in codes originally developed at the U.S. National Laboratories and subsequently released to the general public which are capable of tracking fluid interfaces in a variety of complex fluid flow problems [9; 12; 19; 35; 36]).

In this paper I do not consider the related problem of approximating the movement of the interface in time, for which one would use a *volume-of-fluid advection algorithm*. See [23; 27; 28] for a detailed description and analysis of several such algorithms. In the present paper I only consider the accuracy that one can obtain when using a volume-of-fluid interface reconstruction algorithm to approximate a given *stationary* interface $\mathbf{z}(s)$.

1.2. *Basic assumptions and definitions.* Unless explicitly stated otherwise, I will always assume that the *exact* interface $\mathbf{z}(s) = (x(s), y(s))$ is twice continuously differentiable: $\mathbf{z} \in C^2(\Omega)$. In particular, the derivatives $\dot{x}(s)$, $\dot{y}(s)$, $\ddot{x}(s)$ and $\ddot{y}(s)$ exist and are continuous. I also assume that the curvature $\kappa(s)$ of the interface $\mathbf{z}(s)$ is bounded in Ω, so that there always exists a constant $\kappa_{\max}$ independent of s such that (2) holds.

By the *center cell* C_{ij} I mean the square with side h that contains a portion of the interface $\mathbf{z}(s) = (x(s), y(s))$ for s in some interval, say $s \in (s_l, s_r)$. In what follows I will consider the 3×3 block of square cells B_{ij} — each with side h, surrounding the center cell as shown, for example, in Figure 1. Unless I note otherwise, I will denote the coordinates of the vertical edges of the cells in the 3×3 block B_{ij} centered on the cell C_{ij} by x_{i-2}, x_{i-1}, x_i and x_{i+1} and the horizontal edges of the cells in B_{ij} by y_{j-2}, y_{j-1}, y_j, y_{j+1} as shown, for example, in Figure 1. It will always be the case that

$$x_{i+1} - x_i = h, \qquad x_i - x_{i-1} = h,$$
$$y_{j+1} - y_j = h, \qquad y_j - y_{j-1} = h,$$

and so on, where h is the (nondimensional) grid size.

1.3. *The column sums*. The volume fraction Λ_{ij} in the (i, j)-th cell C_{ij} is a nondimensional way of storing the volume of dark fluid in that cell. Consider the column consisting of C_{ij} and the cells immediately above and below C_{ij}. The *column sum*

$$S_i \equiv \sum_{j'=j-1}^{j+1} \Lambda_{ij'}$$

is a nondimensional way of storing the total volume of dark fluid in those three cells. In order to approximate the portion of the interface $g(x)$ lying in the (i, j)-th cell C_{ij}, I will use the three column sums in the 3×3 block of cells B_{ij} that have C_{ij} in its center to compute the slope m of the piecewise linear approximation $\tilde{g}(x)$ to $g(x)$ (for example, see Figure 1). I use S_{i-1} to denote the column sum to the left of S_i and S_{i+1} to denote the column sum to the right of S_i, so that

$$S_{i-1} \equiv \sum_{j'=j-1}^{j+1} \Lambda_{i-1,j'}, \quad S_{i+1} \equiv \sum_{j'=j-1}^{j+1} \Lambda_{i+1,j'}. \tag{10}$$

Now consider an arbitrary column consisting of three cells with left edge $x = x_i$ and right edge $x = x_{i+1}$. Furthermore, assume that the interface can be written as a function $y = g(x)$ on the interval $[x_i, x_{i+1}]$. Assume also that the interface enters the column through its left edge and exits the column through its right edge and does not cross the top or bottom edges of the column, as is the case with all three columns in the example shown in Figure 1. Then the total volume of dark fluid that occupies the three cells in this particular column and lies below the interface $g(x)$ is equal to the integral of g over the interval $[x_i, x_{i+1}]$. This leads to the following relationship between the column sum and the *normalized*[6] volume of dark fluid in

---

[6]The normalized volume is the nondimensional quantity obtained by dividing the integral of $g(x)$ over the interval $[x_i, x_{i+1}]$ by h^2.

the column:

$$S_i \equiv \sum_{j'=j-1}^{j+1} \Lambda_{ij'} = \frac{1}{h^2} \int_{x_i}^{x_{i+1}} \left(g(x) - y_{j-2}\, h \right) \, dx. \tag{11}$$

I will use the phrase *the i-th column sum S_i is exact* whenever (11) holds, and I will refer to integrals such as the one on the right in (11) as *the normalized integral of g* in that column.

Given the 3×3 block of cells surrounding a cell C_{ij} that contains a portion $y = g(x)$ of the interface, most of the important results in this paper are based on how well the column sums S_{i-1}, S_i and S_{i+1} approximate the normalized integral of g in that particular column. This is because the slope m_{ij} of the piecewise linear approximation to g in C_{ij} will be the divided difference of two of these column sums; that is, m_{ij} is chosen to be one of the three quantities

$$m_{ij}^l = S_i - S_{i-1}, \quad m_{ij}^c = \tfrac{1}{2}(S_{i+1} - S_{i-1}), \quad m_{ij}^r = S_{i+1} - S_i. \tag{12}$$

In particular, if two of the column sums $S_{i+\alpha}$ and $S_{i+\beta}$ where $\alpha, \beta = 1, 0, -1$ and $\alpha \neq \beta$ are exact, then the slope

$$m_{ij} = \frac{(S_{i+\alpha} - S_{i+\beta})}{(\alpha - \beta)} \tag{13}$$

will produce a piecewise linear approximation $\tilde{g}(x)$ to the portion of the interface $g(x)$ in C_{ij} that is second-order accurate in the max norm as shown, for example, in Figure 1.

In order to see why this will be the most accurate choice for the approximate slope m_{ij}, consider the case when the block B_{ij} has two exact column sums as shown in Figure 2. In this example the interface is a line $g(x) = mx + b$. In this particular orientation of the 3×3 block of cells g has two exact column sums; namely, the sums in the first and second columns. It is easy to check that

$$m = \frac{1}{h^2} \int_{x_{i-1}}^{x_i} (g(x) - y_{j-2}h)\, dx$$

$$- \frac{1}{h^2} \int_{x_{i-2}}^{x_{i-1}} (g(x) - y_{j-2}h)\, dx = (S_i - S_{i-1}) = m_{ij}^l,$$

where S_i denotes the column sum associated with the interval $[x_{i-1}, x_i]$ and S_{i-1} denotes the column sum associated with the interval $[x_{i-2}, x_{i-1}]$.

In this example, the divided difference m_{ij}^l of the column sums S_{i-1} and S_i is exactly equal to the slope m of the exact interface. It is *always* the case that when the exact interface is a line one can find an orientation of the 3×3 block of cells such that at least one of the divided differences of the column sums in (12) is exact.
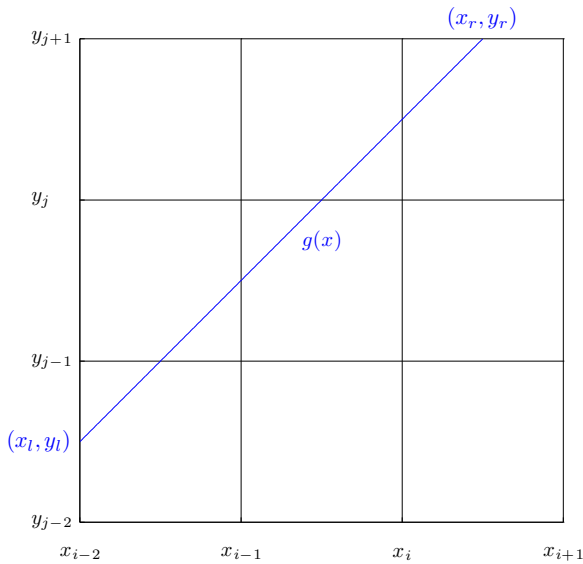
Figure 2.   Here the interface is a line, $g(x) = mx + b$, having two exact column sums (those in the first and second columns). The slope m_{ij}^l from (12) is then exactly equal to the slope m of the interface: $m_{ij}^l = m$. Whenever the exact interface is a line, one can find an orientation of the 3×3 block of cells such that at least one of the divided differences of the column sums in (12) is exact.

For example, in the case shown in Figure 2 one could rotate the 3×3 block of cells 90 degrees clockwise and in this orientation the correct slope to use when forming the piecewise linear approximation $\tilde{g}(x) = m_{ij} + b_{ij}$ would be $m_{ij} = m_{ij}^r$, which again would be exactly equal to the slope m of the exact interface.

However, as I will show in Section 3, there are some instances in which the interface satisfies (3) but the center column sum S_i is not exact. Much of the work in Section 3 is devoted to showing that when the interface satisfies (3), the center column sum S_i are exact to $O(h)$:

$$\frac{1}{h^2} \int_{x_i}^{x_{i+1}} (g(x) - y_{j-2}h)\,dx - S_i = Ch,$$

where $C > 0$ is a constant that is independent of h. Then, in Section 4, I prove that this is sufficient to still obtain second-order accuracy in the max norm.

I am now ready to finish the description of the volume-of-fluid interface reconstruction algorithms that I study in this article. Given an arbitrary interface **z** in the domain Ω, I choose an orientation of the 3×3 block of cells such that at least two of the column sums are sufficiently accurate that one of the divided differences in

(12) satisfies

$$|m_{ij} - g'(x_c)| \le Ch, \tag{14}$$

where C is a constant that is independent of h. In this article I prove that, provided the condition in (3) is satisfied, it is possible to find such an orientation.

1.4. _A brief overview of the structure of this article._ In the next section I begin by proving several lemmas that lead to Theorem 6, which states that if

$$h \le C_h \, (\kappa_{\max})^{-1} \tag{15}$$

where C_h is defined in (4), then the interface can be written as a function of one of the coordinate variables in terms of the other on an interval $[a, b]$ with $|b - a| \ge 4h$. This ensures that, given a cell C_{ij} that contains a portion of the interface, I can always find a 3×3 block of cells centered on the cell C_{ij} in which I can write the interface as a function of one of the variables in terms of the other; for example, $y = g(x)$. To achieve this, it may be necessary to rotate the 3×3 block of cells centered on C_{ij} by 90, 180, or 270 degrees and/or reflect the coordinates about one of the coordinate axes: $x \to -x$ or $y \to -y$. No other coordinate transformations besides one of these three rotations and a possible reversal of one or both of the variables $x \to -x$ and/or $y \to -y$ are required in order for the algorithms studied in this article to converge to the exact interface as $h \to 0$. Furthermore, these coordinate transformations are only used to determine a first-order accurate approximation to the slope of the tangent to the interface $\mathbf{z}$ in the current cell of interest, or equivalently, a first-order accurate approximation m to $g'(x_c)$ in the center cell, as shown, for example, in Figure 1. The grid covering the domain Ω always remains the same.

In particular, if one is using the interface reconstruction algorithm as part of a numerical method to solve a more complex problem than the one posed here (for example, the movement of a fluid interface where the fluid flow is a solution of the Euler or Navier–Stokes equations), it is not necessary to perform these coordinate transformations on the underlying numerical fluid flow solver. Therefore, unless noted otherwise, in what follows I will always write $y = g(x)$ and denote the coordinates of the edges of the cells in the 3×3 block by $x = x_{i-2}, x_{i-1}, x_i, x_{i+1}$ and $y = y_{j-2}, y_{j-1}, y_j, y_{j+1}$, it being implicitly understood that a transformation of the coordinate system as described above may have been performed in order for this representation of the interface to be valid, and that I may have interchanged the names of the variables x and y in order to write the interface as $y = g(x)$.

In Section 2 I will also prove that in the (possibly transformed) coordinates the function $y = g(x)$ that represents the interface satisfies

$$|g'(x)| \le \sqrt{3}, \quad \max_x |g''(x)| \le 8\kappa_{\max}. \tag{16}$$

These inequalities are a part of Theorem 6. I use these bounds to prove several of the results in Sections 3 and 4.

In Section 3 I prove that if h satisfies

$$h \leq \max\{C_h(\kappa_{\max})^{-1}, (\kappa_{\max})^{-2}\},$$

then, using one of the transformations described above, I can find a coordinate frame in which there are at least two columns with column sums $S_{i+\alpha}$ and $S_{i+\beta}$ in the 3×3 block of cells B_{ij} centered on the cell C_{ij} which contains the portion of the interface of interest, such that their divided difference,

$$m_{ij} = \frac{(S_{i+\alpha} - S_{i+\beta})}{(\alpha - \beta)} \quad \text{for } \alpha, \beta = -1, 0, 1 \text{ and } \alpha \neq \beta,$$

satisfies (14).

In Section 4 I use this result to prove Theorem 24, which is the main result of this paper. Namely that $\tilde{g}(x)$ is a second-order accurate approximation to $g(x)$ in I_i in the max norm:

$$|g(x) - \tilde{g}_{ij}(x)| \leq \left(\frac{50}{3}\kappa_{\max} + C_S\right)h^2 \quad \text{for all } x \in I_i = [x_{i-1}, x_i].$$

Here C_S is a constant that is independent of h and the approximate interface $\tilde{g}_{ij}(x)$ is being constructed in the center cell $C_{ij} = [x_{i-1}, x_i] \times [y_{j-1}, y_j]$ of the 3×3 block of cells B_{ij} that contains the portion of the interface that is of interest, as shown, for example, in Figure 1. A corollary of this result is that when the size of the computational grid h is too large

$$h \geq H_{\max}, \tag{17}$$

where $H_{\max}$ is defined in (7), then the convergence rate *may* be less than second-order. Thus, (17) may be used as a criterion for predicting when the computation of the interface may be under-resolved.

2. The first constraint on the grid size h

The principle purpose of this section is to show that for a given interface $\mathbf{z}(s)$ with a maximum curvature $\kappa_{\max}$ there exists a value of the grid size $h = h_{\max}$ such that the interface can be written as a function of one of the coordinate variables in terms of the other in any given 3×3 block of cells B_{ij} of side $h \leq h_{\max}$ centered on a cell C_{ij} that contains a portion of the interface. The main result in this section is Theorem 6, in which I derive the constraint

$$h \leq h_{\max} \equiv C_h(\kappa_{\max})^{-1}, \tag{18}$$

where C_h is the constant defined in (4). I also prove that in the same 3×3 block of cells B_{ij} centered on the cell C_{ij} the bounds in (16) hold.

The constraint in (18) is not sufficient to guarantee that the volume-of-fluid interface reconstruction algorithm will be second-order accurate in the limit as $h \to 0$. In Section 3 below, I will show that this requires a more stringent constraint on h, namely

$$h \le (\kappa_{\max})^{-2}.$$

Suppose that I am interested in a neighborhood of the point $\mathbf{z}(s_0) = (x(s_0), y(s_0)) \equiv (x_0, y_0)$ on the interface[7] and at this point I have

$$\dot{x}^2(s_0) \ge \tfrac{1}{2}. \tag{19}$$

I will now show that in some neighborhood of the point (x_0, y_0) I can represent the interface $(x(s), y(s))$ as the single valued function $y(s) = g(x(s))$. Then, in Lemma 4 I will answer the question: *Over how large an interval $[x_l, x_r]$ where $x_l < x_0 = x(s_0) < x_r$ is this representation of the interface valid?* I will now proceed to address this question.

Let $s_l < s_r$[8] chosen such that s_l is the largest number less than s_0 and s_r is the smallest number greater than s_0 such that

$$\dot{x}^2(s) \ge \tfrac{1}{4} \quad \text{for all } s \in [s_l, s_r]. \tag{20}$$

Given that at the point $\mathbf{z}(s_0)$ the inequality in (19) holds there are two possibilities for the point $\mathbf{z}(s_l)$ (resp. $\mathbf{z}(s_r)$).

(1) At the point $\mathbf{z}(s_l)$ (resp. $\mathbf{z}(s_r)$) I have

$$\dot{x}^2(s_l) = \tfrac{1}{4} \quad \left(\text{resp. } \dot{x}^2(s_r) = \tfrac{1}{4}\right). \tag{21}$$

In this case I can estimate the size of the interval $[x_l, x_0]$ (resp. $[x_0, x_r]$) over which I can represent the interface as a function of one of the coordinate variables in terms of the other, say $y = g(x)$, and bound the first and second derivatives of this function. All of these estimates will be in terms of one quantity; namely, $\kappa_{\max}$, the maximum curvature of the interface.

(2) For all $s < s_0$ (resp. $s > s_0$) I have

$$\dot{x}^2(s) > \tfrac{1}{4},$$

and at some point $\mathbf{z}(s_l)$ (resp. $\mathbf{z}(s_r)$) the interface $\mathbf{z}(s)$ intersects the boundary of the computational domain Ω. In this case the bound in (2) holds from the point x_0 up to the point x_l (resp. x_r) on the boundary. In this case, I can

---

[7] In this section, and this section only, x_0 and y_0 denote a point on the interface $\mathbf{z}(s_0) = (x(s_0), y(s_0)) \equiv (x_0, y_0)$ rather than the location of one of the grid lines in the 3×3 block of cells.

[8] Without loss of generality I can assume that $x(s)$ increases with increasing s, since otherwise the change of variables $s \to -s$ is also a parametrization of the interface by arc length for which $x(s)$ increases with increasing s.

express the interface as a function such as $y = g(x)$ from $x_0 \in [-h/2, h/2]$ all the way to the boundary on the left (resp. right); that is, in the interval $[x_l, x_0]$ (resp. in the interval $[x_0, x_r]$).

Note that since I have assumed that the domain Ω is bounded and that either the interface enters and exits the domain across the boundary or it is a closed curve in Ω, these are the only two possibilities. For if the interface is a closed curve, such as a circle, it must be the case that eventually $\dot{x}(s) \to 0$.

In either case, there is an interval $[x_l, x_r]$ upon which I can express the interface as a function $y = g(x)$ and upon which all of the bounds that I prove below will hold. The only difference between cases (1) and (2) above is that in case (2) one or both of the points x_l and x_r lie on the boundary of the domain.

Since, for the purposes of the proving the lemmas and theorems below, I do not know a priori the distance from x_0 to the boundary, for the remainder of this section I will assume that case (1) above holds and proceed to estimate the size of the intervals $[x_l, x_0]$ and $[x_0, x_r]$ in terms of the bound $\kappa_{\max}$ on the curvature of the interface. This will allow me to explicitly estimate the size of the interval $[x_l, x_r]$ containing the point of interest $(x_0, y_0) \equiv (x(s_0), y(s_0))$ over which I can express the interface as a function $y = g(x)$ and prove explicit bounds on the first and second derivatives of g.

Remark 1. If the inequality in (19) fails to hold at the point $\mathbf{z}(s_0)$ at which I wish to reconstruct the interface, then $\dot{y}^2(s_0) \geq \frac{1}{2}$ instead, since s is arc length and hence $\dot{x}^2(s) + \dot{y}^2(s) = 1$. In this case I instead choose y to be the independent variable and the same analysis will produce the same estimates throughout. Therefore, in all of what follows x will denote the independent variable, it being understood that in some cases y is the correct variable to choose.

Remark 2. The choice of the constant $\frac{1}{2}$ in (19) and the constant $\frac{1}{4}$ in (21) is arbitrary. One could have chosen instead any two constants C_1 and C_2 that satisfy $C_1 > C_2 > 0$ in the proof of Lemma 3. The lemma will continue to hold, but the values of the constants C_h and $h_{\max}$ in Theorem 6 below will change. In other words, all of our results will remain true, albeit with different constants.

I begin by finding a bounds on the second derivatives $\ddot{x}(s)$ and $\ddot{y}(s)$ of the functions $x(s)$ and $y(s)$ in terms of the global bound $\kappa_{\max}$ on the curvature of the interface. I will use these bounds to estimate the size of the intervals $[x_l, x_0]$ and $[x_0, x_r]$ in terms of the intervals $[s_l, s_0]$ and $[s_0, s_r]$, respectively, in the two subsequent lemmas.

Lemma 3 (A bound on $\ddot{x}(s)$ and $\ddot{y}(s)$). *Suppose that I am given a point* $\mathbf{z}(s_0) = (x(s_0), y(s_0))$ *on the interface at which the inequality*

$$\dot{y}^2(s) \leq \tfrac{1}{2} \leq \dot{x}^2(s) \tag{22}$$

holds. Let $s_l < s_0$ be the largest number less than s_0 and $s_r > s_0$ be the smallest number greater than s_0 such that

$$\tfrac{1}{4} \leq \dot{x}^2(s) \quad \left(\text{and hence } \dot{y}^2(s) \leq \tfrac{3}{4}\right) \quad \text{for all } s \in [s_l, s_r]. \tag{23}$$

Then

$$|\ddot{x}(s)| \leq \tfrac{\sqrt{3}}{2}\kappa_{\max} \quad \text{for all } s \in [s_l, s_r]. \tag{24}$$

Similarly, if the roles of $\dot{x}(s)$ and $\dot{y}(s)$ are reversed in the inequalities in Equations (22) and (23) above, then I have

$$|\ddot{y}(s)| \leq \tfrac{\sqrt{3}}{2}\kappa_{\max} \quad \text{for all } s \in [s_l, s_r]. \tag{25}$$

Proof. To begin, recall that since the parameter s is arc length,

$$\dot{x}^2(s) + \dot{y}^2(s) = 1 \tag{26}$$

holds for all s, and hence the curvature $\kappa(s)$ can be written as

$$\kappa(s) = \dot{x}(s)\ddot{y}(s) - \dot{y}(s)\ddot{x}(s) \tag{27}$$

(see [29, page 555]). Differentiating (26) with respect to s I find that

$$\dot{x}(s)\ddot{x}(s) = -\dot{y}(s)\ddot{y}(s), \tag{28}$$

or equivalently

$$-\dot{x}^2(s)\ddot{x}(s) = \dot{y}(s)\dot{x}(s)\ddot{y}(s). \tag{29}$$

Multiplying (27) by $\dot{y}(s)$ I have

$$\dot{y}(s)\kappa(s) = \dot{y}(s)\dot{x}(s)\ddot{y}(s) - \dot{y}^2(s)\ddot{x}(s), \tag{30}$$

and thus, using (29) in (30), I obtain

$$\dot{y}(s)\kappa(s) = -\ddot{x}(s)(\dot{x}^2(s) + \dot{y}^2(s)) = -\ddot{x}(s). \tag{31}$$

Combining (31) and (23) I obtain the following bound on $\ddot{x}(s)$ in terms of the bound $\kappa_{\max}$ on the curvature $\kappa(s)$,

$$|\ddot{x}(s)| = |\dot{y}(s)\kappa(s)| \leq |\dot{y}(s)|\kappa_{\max} \leq \tfrac{\sqrt{3}}{2}\kappa_{\max}.$$

One can use an identical argument to prove the bound on $\ddot{y}(s)$ in (25). □

In the next lemma I explicitly demonstrate how the size of the intervals $[x_l, x_0]$ and $[x_0, x_r]$ depend on the size of the intervals $[s_l, s_0]$ and $[s_0, s_r]$ respectively. In the lemma after that I provide an explicit relationship between the size of the intervals $[s_l, s_0]$ and $[s_0, s_r]$ the bound $\kappa_{\max}$ in (2) on the curvature of the interface.

Lemma 4. *Let* $\mathbf{z}(s_0) = (x(s_0), y(s_0))$ *be a point on the interface at which the inequality*

$$\dot{y}^2(s_0) \leq \tfrac{1}{2} \leq \dot{x}^2(s_0)$$

holds, and let $s_l < s_0$ *be the greatest number less than* s_0 *and* $s_r > s_0$ *the smallest number greater than* s_0 *such that*

$$\tfrac{1}{4} \leq \dot{x}^2(s) \quad \text{for all } s \in [s_l, s_r]. \tag{32}$$

Then, letting $x_l \equiv x(s_l)$, $x_0 \equiv x(s_0)$, *and* $x_r \equiv x(s_r)$, *the following inequalities hold*:

$$\tfrac{1}{2}|s_0 - s_l| \leq |x_0 - x_l| \leq |s_0 - s_l|, \quad \tfrac{1}{2}|s_r - s_0| \leq |x_r - x_0| \leq |s_r - s_0|. \tag{33}$$

Proof. I prove that the inequalities involving s_l are true. The proof of the other pair of inequalities is identical. By the mean-value theorem I have

$$x_0 - x_l = \dot{x}(\tilde{s})(s_0 - s_l) \quad \text{for some} \quad \tilde{s} \in (s_0, s_l). \tag{34}$$

Since both (26) and (32) hold I have $\tfrac{1}{4} \leq \dot{x}^2(s) \leq 1$ for all $s \in [s_l, s_r]$, and hence

$$\tfrac{1}{2} \leq |\dot{x}(s)| \leq 1 \quad \text{for all } s \in [s_l, s_r]. \tag{35}$$

Combining (34) and (35) I obtain

$$\tfrac{1}{2}|s_0 - s_l| \leq |x_0 - x_l| \leq |s_0 - s_l|,$$

as claimed. $\qquad\qquad\qquad\qquad\qquad\qquad\qquad\qquad\qquad\qquad\qquad\qquad$ □

But how large are the intervals $[s_l, s_0]$ and $[s_0, s_r]$ in terms of the physical coordinates x and y? The following lemma addresses this question.

Lemma 5. *Let* $\mathbf{z}(s_0) = (x(s_0), y(s_0))$ *be a point on the interface at which the inequality*

$$\dot{y}^2(s_0) \leq \tfrac{1}{2} \leq \dot{x}^2(s_0) \tag{36}$$

holds. If $s_l < s_0$ *is the greatest number less than* s_0 *and* $s_r > s_0$ *is the smallest number greater than* s_0 *such that*

$$\dot{x}^2(s_l) = \tfrac{1}{4} = \dot{x}^2(s_r), \tag{37}$$

then the distances $|s_r - s_0|$ *and* $|s_0 - s_l|$ *satisfy*

$$|s_0 - s_l| \geq \frac{\sqrt{2} - 1}{\sqrt{3}} (\kappa_{\max})^{-1}, \quad |s_r - s_0| \geq \frac{\sqrt{2} - 1}{\sqrt{3}} (\kappa_{\max})^{-1}. \tag{38}$$

Proof. I will prove the first inequality; the proof of the second is identical. Let $\dot{x}_l = \dot{x}(s_l)$ and $\dot{x}_0 = \dot{x}(s_0)$. By the mean-value theorem I have $\dot{x}_0 - \dot{x}_l = \ddot{x}(\tilde{s})(s_0 - s_l)$ for some $\tilde{s} \in (s_0, s_r)$, and hence

$$|\dot{x}_0 - \dot{x}_l| = |\ddot{x}(\tilde{s})||s_0 - s_l| \leq \tfrac{\sqrt{3}}{2}|s_0 - s_l|\kappa_{\max}, \tag{39}$$

where the inequality in (39) follows from (24). Thus

$$|s_0 - s_l| \geq \frac{2}{\sqrt{3}} |\dot{x}_0 - \dot{x}_l| (\kappa_{\max})^{-1}. \tag{40}$$

Now from (36) and (37), I have $|\dot{x}_l| = \frac{1}{2}$ and $|\dot{x}_0| \geq \frac{1}{\sqrt{2}}$, and hence

$$|\dot{x}_0 - \dot{x}_l| \geq \frac{\sqrt{2} - 1}{2}. \tag{41}$$

Combining (40) and (41) I obtain, as needed,

$$|s_0 - s_l| \geq \frac{2}{\sqrt{3}} |\dot{x}_0 - \dot{x}_l| (\kappa_{\max})^{-1} \geq \frac{\sqrt{2} - 1}{\sqrt{3}} (\kappa_{\max})^{-1}, \qquad \square$$

I am now prepared to explicitly demonstrate the relationship between the maximum allowable cell size $h_{\max}$ and the bound on the curvature $\kappa_{\max}$ such that for all $h \leq h_{\max}$ the inequality in (20) holds for all x in the interval $[x_0 - 2h, x_0 + 2h]$, and hence the interface can be represented as a single-valued function $y = g(x)$ in the 3×3 block of cells B_{ij} of side h surrounding the cell C_{ij} containing the point (x_0, y_0) on the interface.

Theorem 6. *Suppose that I wish to reconstruct the interface in a neighborhood of the point* $\mathbf{z}(s_0) = (x(s_0), y(s_0))$ *and that at this point*

$$\dot{y}^2(s_0) \leq \tfrac{1}{2} \leq \dot{x}^2(s_0). \tag{42}$$

Let $s_l < s_0$ *be the greatest number less than* s_0 *and* $s_r > s_0$ *be the smallest number greater than* s_0 *such that*

$$\tfrac{1}{4} \leq \dot{x}^2(s) \quad \text{for all } s \in [s_l, s_r]. \tag{43}$$

Let $x_0 = x(s_0)$ *and let*

$$h_{\max} = C_h (\kappa_{\max})^{-1}, \tag{44}$$

where

$$C_h \equiv \frac{\sqrt{2} - 1}{4\sqrt{3}} \tag{45}$$

is the constant defined in (4). *Then the interface can be represented as a single-valued function* $y = g(x)$ *on the interval* $[x_0 - 2h_{\max}, x_0 + 2h_{\max}]$. *Furthermore,*

$$\max_{x \in [a,b]} |g'(x)| \leq \sqrt{3} \tag{46}$$

and

$$\max_{x \in [a,b]} |g''(x)| \leq 8\kappa_{\max} \tag{47}$$

where $a = x_0 - 2h_{\max}$ *and* $b = x_0 + 2h_{\max}$.

Remark 7. As a consequence of this theorem, if the point $\mathbf{z}_0 = \mathbf{z}(s_0)$ lies in some cell C_{ij} of side $h \leq h_{\max}$, then the interface can be represented as a single-valued function $y = g(x)$ throughout the 3×3 block B_{ij} of square cells of side h surrounding C_{ij} and the bounds in (46) and (47) hold throughout B_{ij}.

Remark 8. It is apparent that interchanging the roles of $x(s)$ and $y(s)$ in Lemmas 3–5 and Theorem 6 above will show that the interface can be represented as a single-valued function $x = G(y)$ throughout the 3×3 block B_{ij} of square cells of side h surrounding C_{ij} and the bounds in (46) and (47) hold throughout the B_{ij} with x replaced by y and g replaced by G.

Proof. Let $x_l = x(s_l)$ and $x_r = x(s_r)$. Since, by the implicit function theorem, the interface can be represented as a single-valued function $y = g(x)$ on any interval over which $\dot{x}^2(s) \geq \frac{1}{4} \neq 0$, it follows immediately from the assumption in (43) that the interface $\mathbf{z}(s) = (x(s), y(s))$ can be written as $(x(s), g(x(s)))$ for all $s \in [s_l, s_r]$; or, equivalently, as $(x, g(x))$ for all $x \in [x_l, x_r]$.

Now I need to prove that $[x_0 - 2h_{\max}, x_0 + 2h_{\max}] \subseteq [x_l, x_r]$, or equivalently, that

$$x_l \leq x_0 - 2h_{\max} \tag{48}$$

and

$$x_r \geq x_0 + 2h_{\max}. \tag{49}$$

To see that (48) holds note that (33) and (38) imply

$$|x_0 - x_l| \geq \tfrac{1}{2}|s_0 - s_l| \geq \frac{\sqrt{2} - 1}{\sqrt{3}}(\kappa_{\max})^{-1} = \frac{\sqrt{2} - 1}{2\sqrt{3}}(\kappa_{\max})^{-1} = 2h_{\max}.$$

Since $x_0 - x_l > 0$, Equation (48) follows immediately. The proof of (49) is nearly identical.

To see that (46) holds for $x \in [x_l, x_r]$ note that from (43) I have

$$\frac{1}{\dot{x}^2(s)} \leq 4 \quad \text{for all } s \in [s_l, s_r]. \tag{50}$$

Furthermore, since s is arc length, I know that $\dot{x}^2(s) + \dot{y}^2(s) = 1$ for all s, and hence (43) also implies that

$$\dot{y}^2(s) \leq \tfrac{3}{4} \quad \text{for all } s \in [s_l, s_r]. \tag{51}$$

Combining (50) and (51) yields

$$\left|g'(x(s))\right|^2 = \left|\frac{\dot{y}^2(s)}{\dot{x}^2(s)}\right| \leq 3, \tag{52}$$

from which the expression in (46) follows immediately.

To see that (47) holds on the interval $[x_0 - 2h_{\max}, x_0 + 2h_{\max}]$, write the curvature of the interface $\kappa(x)$ in terms of the first and second derivatives of g [29, page 555]:

$$\kappa(x) = \frac{g''(x)}{\left(1 + g'(x)^2\right)^{3/2}}. \tag{53}$$

The inequality in (47) follows immediately from the fact that (52) holds on $x \in [x_0 - 2\,h_{\max}, x_0 + 2\,h_{\max}]$. $\qquad\square$

3. The accuracy of the column sums in a 3 × 3 block of cells

Notation. In this section I will often denote the edges of the 3 × 3 block of cells by x_0, x_1, x_2, x_3 and y_0, y_1, y_2, y_3 as shown, for example, in Figure 3, rather than x_{i-2}, x_{i-1}, x_i, x_{i+1} and y_{j-2}, y_{j-1}, y_j, y_{j+1}.

It is important to note that there is no bound of the form (3) that will ensure that the interface will always have at least two exact column sums in any of the
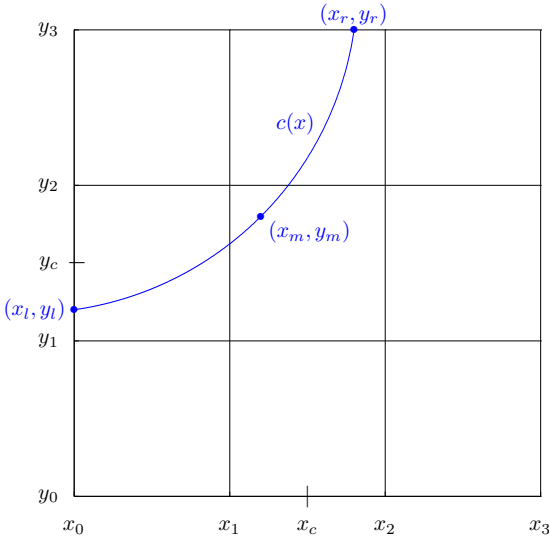
Figure 3. An example of a circular interface $c(x)$ that satisfies (3), but for which the center column sum is not exact in any of the four standard orientations of the grid. Hence, any approximation m to the slope $c'(x_c)$ of the form (13) will perforce have a nonexact column sum S_i. Theorem 15 shows that the error between the sum S_i and the normalized integral of c over the second column is $O(h)$ (that is, (3) implies that (54) holds). Theorem 23 shows that this suffices to prove $|m - c'(x_c)| = O(h)$. Finally, Theorem 24 shows that this yields an approximate interface $\tilde{g}(x)$ which is a second-order accurate approximation of $c(x)$ in the max norm.

four standard orientations of the grid. The argument is as follows. Consider the curve shown in Figure 3, where I have chosen h so that $(\sqrt{h})^{-1} \leq C_h h^{-1}$. Let $0 < \epsilon < h$ be a small parameter. I can always find a circle $c(x)$[9] that passes through the three noncollinear points $(x_l, y_l) = (x_0, y_1 + \epsilon)$, $(x_m, y_m) = (x_1 + \epsilon, y_2 - \epsilon)$ and $(x_r, y_r) = (x_2 - \epsilon, y_3)$ as shown in the figure. As $\epsilon \to 0$ the arc of the circle passing through (x_l, y_l), (x_m, y_m) and (x_r, y_r) tends to the chord connecting (x_l, y_l) and (x_r, y_r), which, since the curvature of the chord is 0, implies that the radius R of the circle tends to ∞. Therefore, for some $\epsilon > 0$, the radius will satisfy $R \geq \sqrt{h}$, or equivalently, $\kappa_{\max} = R^{-1} \leq (\sqrt{h})^{-1}$, and hence the circle satisfies (3). However, since by construction $y_1 < y_l$ and $x_r < x_2$, the center column sum will not be exact in any of the four standard orientations of the block B_{ij}. Consequently, if one wishes to construct an approximation to $c(x)$ based solely on the volume fraction information contained in the 3×3 block B_{ij} centered on the cell C_{ij} containing the point (x_m, y_m), the best result that one can hope for is that the center column sum S_i is exact to $O(h)$.

Much of the work in this section is devoted to showing that when cases such as the one shown in Figure 3 occur, the error between the column sum S_i and the normalized integral of the interface in that column is $O(h)$:

$$\left| S_i - \frac{1}{h^2} \int_{I_i} \left(g(x) - y_{j-2} h \right) dx \right| \leq Ch, \qquad (54)$$

where the constant $C > 0$ is independent of h. In Section 4 I prove that this is sufficient to ensure that the approximations

$$m_{ij}^l = (S_i - S_{i-1}), \quad m_{ij}^r = (S_{i+1} - S_i)$$

to $g'(x_c)$ are still first-order accurate, provided that the column sum S_{i-1} (resp. S_{i+1}) is exact. This fact is essential to the proof of Theorem 24, which is the main result of this paper; namely, that the volume-of-fluid approximation $\tilde{g}(x)$ to the interface $g(x)$ is second-order accurate in the max norm.

In this regard, I introduce the following terminology.

Definition 9. Let $C > 0$ be a constant that is independent of h and let S_i denote the column that is made up of the three cells that are centered on the cell $C_{ij} = [x_{i-1}, x_i] \times [y_{j-1}, y_j]$ in which the interface will be reconstructed. Then I will say that *the i-th column sum S_i is exact to $O(h)$ if and only if* (54) holds.

The main result in this section is Theorem 10; that a *well-resolved* interface has two column sums that are exact to $O(h)$. In other words, given a function g that satisfies (3), one will always be able to find two columns whose divided difference

---

[9]When the exact interface is a circle, I will usually denote it by $c(x)$, as I have done in Figure 3. Otherwise, I always denote the exact interface by $g(x)$.

as defined in (12) will yield a first-order accurate approximation m to $g'(x_c)$ where $x_c = (x_1 + x_2)/2$. This — together with the fact that I know the exact volume of fluid in the center cell — will allow me to construct a piecewise linear approximation $\tilde{g}(x)$ to the interface in that cell which is second-order accurate in the max norm.

I have chosen to present the results in the remainder of this section (and only in this section) in "top down" form. In other words, I state the main result first and prove it, in part, using the results of lemmas and theorems that I state and prove later in the section. I have chosen to structure the paper in this manner because I believe that this makes it much easier for the reader to follow the motivation for the various minor results that I need in order to prove the main results of the section.

3.1. *Assumptions concerning the interface function g.*

In what follows, when I speak about the interface entering and exiting the 3×3 block of cells B_{ij}, I am only concerned with the *last* time that it enters B_{ij} before entering the center cell C_{ij} of the block B_{ij} and the *first* time that it exits B_{ij} after having exited the center column S_i of B_{ij}. As will be apparent from the material below, the condition in (3) prevents a C^2 function of x from entering B_{ij} through one of its edges, passing through the center cell C_{ij}, exiting B_{ij} and then turning around and reentering B_{ij} as shown, for example, in Figure 4. The critical assumptions are that the interface must be a C^2 function of x in some domain

$$D = [x_{i-2}, x_{i+1}] \times [y_b, y_t] \subset \Omega$$
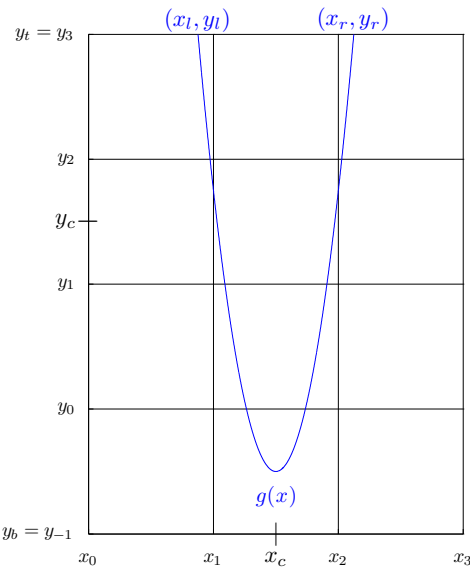
Figure 4. Here $h = 1$ and the interface is the parabola $g(x) = a(x - x_c)^2 - h/2$ with $a = 9$. The maximum curvature $\kappa_{\max} = 18$ exceeds $(\sqrt{h})^{-1} = 1$, so g does not satisfy (3). The interface enters the 3×3 block of cells B_{ij} through the top edge of the first column, passes through the center cell C_{ij}, exits B_{ij} through the bottom edge of the center column (that is, the line $y = y_0$), and then passes through B_{ij} again; the second path being symmetric to the first. In general, as $h \to 0$ the constraint $\kappa_{\max} \leq (\sqrt{h})^{-1}$ on the curvature ensures that the interface does not have "hairpin" turns on the scale of the 3×3 block of cells B_{ij}. A finer grid (that is, a smaller h) is required in order to resolve curves such as the one illustrated here.

with $y_b \leq y_{j-2} < y_{j+1} \leq y_t$ that contains the 3×3 block B_{ij} (see Figure 4 again), and that the interface must satisfy the constraint on the curvature in (3). This precludes the interface from folding back upon itself on scales that are $O(h)$.

Theorem 10 (A well-resolved interface has two column sums that are exact to $O(h)$). *Consider the 3×3 block of square cells B_{ij}, each with side h, centered on the cell C_{ij} through which the interface $\mathbf{z}(s)$ passes. Assume that in some domain $D = [x_{i-2}, x_{i+1}] \times [y_b, y_t] \subseteq \Omega$ with $y_b \leq y_{j-2} < y_{j+1} \leq y_t$ (resp. $D = [x_b, x_t] \times [y_{j-2}, y_{j+1}] \subseteq \Omega$ with $x_b \leq x_{i-2} < x_{i+1} \leq x_t$) that contains the 3×3 block of cells B_{ij} the interface $\mathbf{z}(s)$ can be represented as a function $y = g(x)$ (resp. $x = G(y)$) with $g \in C^2[x_{i-2}, x_{i+1}]$ (resp. $G \in C^2[y_{j-2}, y_{j+1}]$). Furthermore, assume that the interface $\mathbf{z}(s)$ satisfies the constraint on the curvature in Equation (3). Then in one of the standard orientations of the grid (that is, rotation of the block by 0, 90, 180, or 270 degrees and/or interchanging the arc length parameter s with $s' = -s$) the interface has at least two column sums that are either exact or exact to $O(h)$.*

The remainder of Section 3 is concerned with proving Theorem 10 via a sequence of lemmas and theorems. In proving this theorem I will use symmetry arguments such as the one demonstrated in Figure 5. In the following *symmetry lemma*, I show that when the constraint on the curvature in Equation (3) holds there are only four canonical ways the interface can enter the 3×3 block of cells B_{ij}, pass through the center cell C_{ij} and then exit B_{ij}. In the remainder of the lemmas and theorems in this section I will show that, given the assumptions of Theorem 10, two of these cases are not possible and in the other two cases either there are at least two distinct column sums in B_{ij} that are exact to $O(h)$ or the particular interface configuration is not consistent with the hypotheses of Theorem 10.

The purpose of the symmetry lemma is to avoid having to prove that Theorem 10 holds for every possible way in which the interface can enter the 3×3 block of cells B_{ij}, pass through the center cell C_{ij} and then exit B_{ij}, and reduce all of these possible cases to the four canonical cases mentioned above. In the proof of the symmetry lemma, I will argue that one particular interface configuration is *equivalent* to another, say configuration 1 is equivalent to configuration 2, in the sense that the argument I use to prove Theorem 10 is true for configuration 1 can also be used to prove that the theorem is true for configuration 2. In order to see that configurations 1 and 2 are equivalent I will argue that by

(1) rotating the block B_{ij} by 90, 180, 270 degrees, and/or

(2) interchanging the arc length parameter s with $s' = -s$, and/or

(3) reflecting the block B_{ij} about one of the centerlines $x = x_c = (x_1 + x_2)/2$ or $y_c = (y_1 + y_2)/2$.
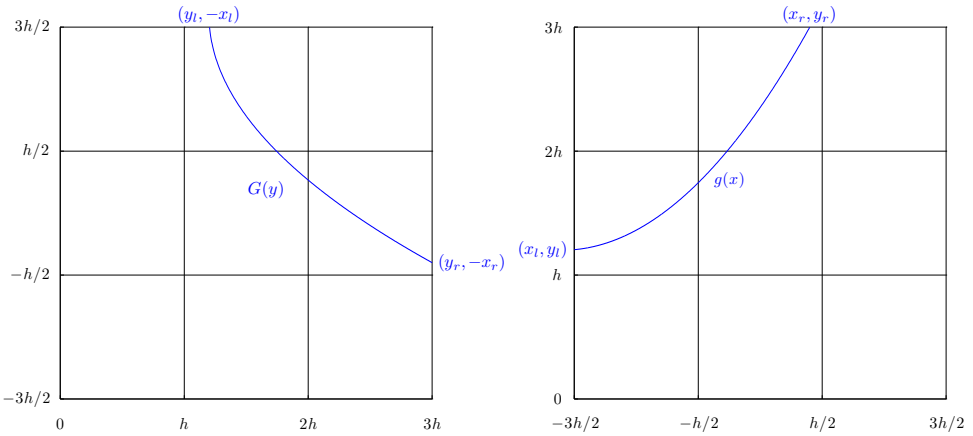
Figure 5. The same interface viewed in two different orientations. Left: In this orientation the interface, written as $-x = G(y)$, has one exact column sum (the third); it enters through the top edge of the center column and exits through the right-hand edge of B_{ij}, so the hypotheses of Theorem 15 do not apply. Right: Upon rotation of the grid clockwise by 270 degrees the interface, now described by $y = g(x)$ (g being the inverse funtion of G, which is strictly monotonic), also has one exact column sum; but here it does satisfy the hypotheses of Theorem 15, so S_i is exact to $O(h)$.

I can use the same proof for configuration 2 as for configuration 1. An example is seen in Figure 5. Note that it is not necessary to reflect the block B_{ij} about either of the centerlines $x = x_c$ or $y = y_c$ in order to determine the approximate slopes m_{ij}^l, m_{ij}^c and m_{ij}^r defined in (12). I only use reflection of the block about one of the lines $x = x_c$ or $y = y_c$ in order to simplify the proof of the symmetry lemma and hence, of Theorem 10.

Symmetry Lemma. *Assume that the hypotheses of Theorem 10 hold. Since the curvature of the interface* $\mathbf{z}(s)$ *is an intrinsic property of the interface, and hence does not depend on the orientation of the coordinate system that I choose to work in, I only need to prove that the conclusions of Theorem 10 hold in the following four cases*:

I. *The interface* $\mathbf{z}$ *enters the* 3×3 *block of cells across its top edge, passes through the center cell and exits the* 3×3 *block of cells across its top edge.*

II. *The interface* $\mathbf{z}$ *enters the* 3×3 *block of cells across its left edge, passes through the center cell and exits the* 3×3 *block of cells across its right edge.*

III. *The interface* **z** *enters the* 3×3 *block of cells across its top edge, passes through the center cell and exits the* 3×3 *block of cells across its bottom edge.*

IV. *The interface* **z** *enters the* 3×3 *block of cells across its left hand edge, passes through the center cell and exits the* 3×3 *block of cells across its top edge.*

Proof. As already noted, without loss of generality I may assume that the arc length s has been chosen so that the interface is traversed from left to right as s increases. In particular, this implies that I do not need to consider any case in which the interface enters the 3×3 block of cells across its right edge.

To assist the reader in following the argument that I need only consider cases I–IV, the following is a list of *all* of the ways in which the interface g can enter and exit the 3×3 block of cells together with which of cases I–IV it is equivalent to.

(1) The interface **z** enters the 3×3 block of cells across the left edge and exits across:

    (a) The left edge. This violates the assumption that the cell size h is sufficiently small that the interface can be written as a *function* of one of the coordinate variables in terms of the other in the 3×3 block of cells B_{ij}.

    (b) The right edge. This is case II. Since, the interface can be written as a function on the 3×3 block of cells B_{ij} and the *first time* that the interface exits B_{ij} is across the right-hand edge, it has three exact column sums as shown, for example, in Figure 1. Thus, I have just proved that Theorem 10 holds for case II.

    (c) The top edge. This is case IV in the statement of the Symmetry Lemma and is the subject of Lemma 13 and Theorem 15 below. (All of the work in Section 3.2 below is concerned with proving this case when the interface is an increasing, monotonic function of x.)

    (d) The bottom edge. After reflection about the line $y = y_c$ and reversal of the arc length parameter $s \rightarrow s' = -s$ this is equivalent to (1c) immediately above and hence falls under case IV in the statement of the Symmetry Lemma.

(2) The interface **z** enters the 3×3 block of cells across the top edge and exits across:

    (a) The left edge. Upon reversal of the arc length parameter $s \rightarrow s' = -s$ this case is equivalent to case (1c), and hence is equivalent to case IV in the statement of the theorem.

    (b) The right edge. Upon reflection of the 3×3 block of cells about the midline $x = x_c$ this case is equivalent to case (1c), and hence is equivalent to case IV in the statement of the theorem.

(c) The bottom edge. This is case III of the Symmetry Lemma. It has two subcases:

  (i) The interface $y = g(x)$ is strictly monotonic in the 3×3 block of cells B_{ij}, and therefore it is invertible. Rotating the 3×3 block of cells 90 degrees counterclockwise yields case (1b) and hence this case is equivalent to case II of the Symmetry Lemma. I have already proven that Theorem 10 holds in this case.

  (ii) The interface $\mathbf{z}$ is not strictly monotonic in the 3×3 block of cells B_{ij}. In Lemma 12 I will prove that this case cannot occur.

(d) The top edge. This is case I of the symmetry lemma. In Lemma 11 I will prove that the condition on the maximum curvature $\kappa_{\max}$ in Equation (3) prevents this case from occurring.

(3) The interface $\mathbf{z}$ enters the 3×3 block of cells B_{ij} across the bottom edge and exits across:

(a) The left edge. After rotation of the block B_{ij} clockwise by 90 degrees this case is equivalent to case (1c), and hence is equivalent to case IV of the symmetry lemma.

(b) The right edge. After rotation of the block B_{ij} by 180 degrees and reversal of the arc length parameter $s \rightarrow s' = -s$ this case is equivalent to case (1c), and hence is equivalent to case IV of the symmetry lemma.

(c) The bottom edge. After rotation of the block B_{ij} by 180 degrees and reversal of the arc length parameter $s \rightarrow s' = -s$ this case is equivalent to (2d) which is case I of the symmetry lemma, which I prove cannot occur.

(d) The top edge. After rotation of the block B_{ij} by 180 degrees and reversal of the arc length parameter $s \rightarrow s' = -s$ this case is equivalent to (2c) above.

(4) The interface $\mathbf{z}$ enters the 3×3 block of cells B_{ij} across the right-hand edge and exits across:

(a) The right edge. As in case (1a) above, this violates the assumption that the cell size h is sufficiently small that the interface can be written as a function in the block B_{ij} and hence, this case is not allowed.

(b) The left edge.

(c) The bottom edge.

(d) The top edge.

  In each of cases 4(b-d) I can change the parametrization of the interface by interchanging the arc length parameter s with $s' = -s$ so that the interface enters the 3×3 block of cells B_{ij} across its left, bottom, or top edge respectively and exits B_{ij} across its right edge. Therefore, cases 4(b-d) are equivalent to cases 1(b), 3(b), and 2(d), respectively.   □

In order to prove that if the interface satisfies the hypotheses of Theorem 10, then it has at least two column sums that are exact to $O(h)$, I will often need to separate the proof into two parts:

A. The interface g is a strictly monotonic function on the interval under consideration.

B. The interface g is not a strictly monotonic function on the interval under consideration.

Recall that a function $g(x)$ is *strictly monotonic* on the interval $[a, b]$ if and only if $x < y \implies g(x) < g(y)$ for all $x, y \in [a, b]$. In the following, when I refer to the interface g as being strictly monotonic or not strictly monotonic, the interval $[a, b]$ is implicitly understood to be $[x_0, x_3]$; that is, the bottom edge of the 3×3 block of cells B_{ij} under consideration.

Recall that ξ is called a *critical point* of the function g if and only if $g'(\xi) = 0$. If the function g is a strictly monotonic function on $[x_0, x_3]$, then it *cannot* have a critical point in $[x_0, x_3]$. In the simplest cases, if g is strictly monotonic then, since it is invertible, the 3×3 grid can be rotated by 90 degrees and an interface that has only one or no exact column sums in the original orientation will have two or three exact column sums in the new orientation. However in one case — namely, the one shown in Figure 5 — the lack of a critical point makes it much more difficult to prove that the interface has at least two column sums that are exact to $O(h)$. The existence of a critical point $\xi \in [x_0, x_3]$ greatly simplifies the proof of Lemmas 11–13. In fact, as will become apparent from the proofs of these lemmas, the existence of a critical point $\xi \in [x_0, x_3]$ is sufficient to force the middle column sum S_i to be exact.

Lemma 11 (Case I of the Symmetry Lemma cannot occur). *Let $g \in C^2[x_0, x_3]$ be a nonmonotonic function that satisfies the assumptions of Theorem 10. Then case I of the symmetry lemma cannot occur; the interface cannot enter the 3×3 block of cells B_{ij} across its top edge at some point (x_l, y_3), pass through the center cell C_{ij} of B_{ij}, and exit B_{ij} across its top edge at some point (x_r, y_3).*

Proof. Since g is assumed to cross the line $y = y_3$ twice in the interval $[x_0, x_3]$ it is not monotonic, and since g must pass through the center cell of the 3×3 block, it follows that g must have at least one critical point $\xi \in [x_0, x_3]$ such that $g'(\xi) = 0$ and $y_3 - g(\xi) > h$. There are two cases:

A. $x_3 - \xi \le 3h/2$; that is, ξ lies to the right of the midline $x = x_c$ of the block B_{ij}.

B. $x_3 - \xi > 3h/2$; that is, ξ lies to the left of the midline $x = x_c$ of the block B_{ij}.

I will prove the theorem for case A. I will then indicate the changes one needs to make in the proof of case A in order to prove case B. Consider the *parabolic*

comparison function p defined by

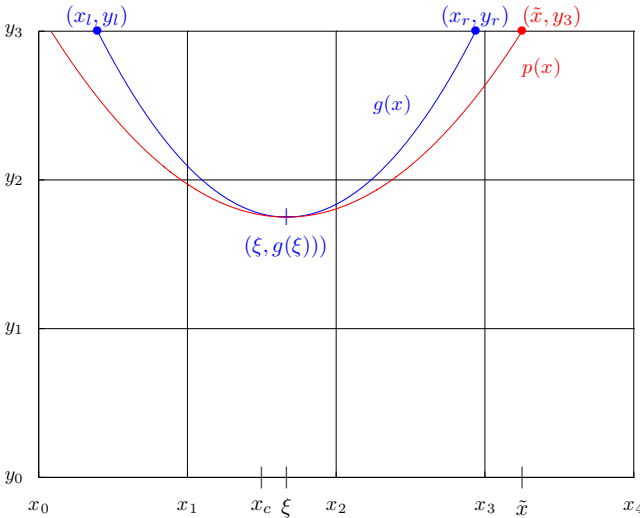$$p(x) = a(x - \xi)^2 + g(\xi),$$

where the coefficient a is given by

$$a = \frac{y_3 - g(\xi)}{(\tilde{x} - \xi)^2} \tag{55}$$

and $\tilde{x} = x_3 + h/4$. See Figure 6 for an example. Note that a was chosen so that

$$p(\tilde{x}) = g(x_r) = y_3, \qquad p'(\xi) = g'(\xi) = 0. \tag{56}$$

Since $g(x_r) = y_3$ and p is a monotone increasing function for $x > \xi$, and $\xi < x_r < \tilde{x}$, I must have $g(x_r) > p(x_r)$. Thus, the difference $f(x) = g(x) - p(x)$ between g and p satisfies

$$f(\xi) = g(\xi) - p(\xi) = 0, \quad f'(\xi) = g'(\xi) - p'(\xi) = 0, \quad f(x_r) = g(x_r) - p(x_r) > 0. \tag{57}$$

Figure 6. An example in which the interface $g(x)$ enters the top edge of the 3×3 block of cells B_{ij} at the point $(x_l, y_l) = (x_l, y_3)$, passes through the center cell C_{ij} and leaves B_{ij} at the point $(x_r, y_r) = (x_r, y_3)$. The function $p(x)$ is the parabolic comparison function that I use for this particular interface in the proof of case A of Lemma 11. The presence of a critical point $(\xi, g(\xi)) \in B_{ij}$ with $g(\xi) < y_2$ is essential to the successful use of a parabolic comparison function in the proof of Lemma 11.

The first and last of these equations imply there exists $\zeta \in [\xi, x_r]$ such that

$$f'(\zeta) = g'(\zeta) - p'(\zeta) > 0, \tag{58}$$

and this, together with the middle equation in (57), imply there exists $\eta \in [\xi, \zeta]$ such that

$$f''(\eta) = g''(\eta) - p''(\eta) > 0. \tag{59}$$

In other words,

$$g''(\eta) > p''(\eta) = 2a \quad \text{for some } \eta \in [\xi, \zeta]. \tag{60}$$

Since $x_3 - \xi \le 3h/2$, it follows that $\tilde{x} - \xi \le 7h/4$, and hence that

$$\frac{1}{(\tilde{x} - \xi)^2} \ge \frac{16}{49h^2}.$$

This inequality, together with $y_3 - g(\xi) > h$, imply

$$g''(\xi) > 2a = 2\frac{(y_3 - g(\xi))}{(\tilde{x} - \xi)^2} > \frac{32h}{49h^2} > \frac{32}{49h}.$$

From (47), I have

$$\max_{x \in [x_0, x_3]} |g''(x)| \le 8\kappa_{\max},$$

and hence $\kappa^g(\xi) \ge g''(\xi)/8$ where $\kappa^g(x)$ denotes the curvature of the interface $g(x)$ at the point $(x, g(x))$. Thus

$$\kappa^g(\xi) \ge \frac{g''(\xi)}{8} > \frac{4}{49h} > \frac{4}{52h} = \frac{1}{13h}. \tag{61}$$

Since $C_h = \frac{\sqrt{2}-1}{4\sqrt{3}} < \frac{1}{16}$, it follows from (61) that

$$\kappa^g_{\max} \ge \kappa^g(\xi) > \frac{1}{13h} > \frac{C_h}{h}.$$

Hence, the interface does not satisfy the assumption (3) and thus this interface configuration cannot occur.

In the event that case B holds, replace (x_r, y_3) with (x_l, y_3), set $\tilde{x} = x_0 - h/4$, etc., and the proof that case I of the symmetry lemma cannot occur when $x_3 - \xi > 3h/2$ (case B) is essentially identical to the proof when $x_3 - \xi \le 3h/2$ (case A). $\square$

Recall that in the proof of the Symmetry Lemma, I showed that case II will always have three exact column sums. Hence case II has already been proved. Therefore, I must now consider case III of the Symmetry Lemma. In the proof of that case, I showed that when the interface function g is strictly monotonic it is equivalent to case II of the Symmetry Lemma, so it also has three exact column sums. Therefore, I only need to consider the nonmonotonic version of case III.

Lemma 12 (Nonmonotonic version of case III of the Symmetry Lemma). *Let $g \in C^2[x_0, x_3]$ be a nonmonotonic function satisfying the assumptions of Theorem 10. Then case III of the Symmetry Lemma cannot occur; that is, the interface cannot enter the 3×3 block of cells B_{ij} across its top edge at some point (x_l, y_3), pass through the center cell C_{ij} of B_{ij}, and exit B_{ij} across its bottom edge at some point (x_r, y_0) with $x_0 \le x_l < x_r \le x_3$.*

Proof. I will show that if the interface g enters the 3×3 block of cells B_{ij} across its top edge, passes through the center cell C_{ij} of B_{ij}, and exits B_{ij} across its bottom edge, then it cannot satisfy

$$\kappa_{\max}^g \le C_h h^{-1} \tag{62}$$

and hence it fails to satisfy the first constraint in (3).

First note that since g is nonmonotonic there is at least one point $\xi \in [x_0, x_3]$ such that $g'(\xi) = 0$. As in the proof of Lemma 11 there are two cases: A and B. However, in this proof I must also consider two subcases of each of these cases:

A. The points ξ and x_3 satisfy $x_3 - \xi \le 3h/2$ and one of the following two conditions hold:

  (i) $y_3 - g(\xi) > h$ (ii) $y_3 - g(\xi) \le h$

B. The points ξ and x_3 satisfy $x_3 - \xi > 3h/2$ and one of the following two conditions hold:

  (i) $y_3 - g(\xi) > h$ (ii) $y_3 - g(\xi) \le h$

I will prove the lemma for case B(i). The proofs of the other three cases are nearly identical.

Therefore, assume that $x_3 - \xi > 3h/2$ and $y_3 - g(\xi) > h$ both hold and consider the parabolic comparison function

$$p(x) = a(x - \xi)^2 + g(\xi)$$

where the coefficient a is defined by

$$a = \frac{3h - g(\xi)}{(\tilde{x} - \xi)^2} \tag{63}$$

and $\tilde{x}$ is defined by $\tilde{x} = x_0 - h/4$. Note that a was chosen so that

$$p(\tilde{x}) = y_3 = 3h, \quad p'(\xi) = g'(\xi) = 0. \tag{64}$$

Since $\tilde{x} < x_l < \xi$ and p is a monotone decreasing function for $x < \xi$, I must have $g(x_l) > p(x_l)$ as shown in Figure 7. Thus, the difference $f(x) = g(x) - p(x)$ between g and p satisfies

$$f(\xi) = g(\xi) - p(\xi) = 0, \quad f'(\xi) = g'(\xi) - p'(\xi) = 0, \quad f(x_l) = g(x_l) - p(x_l) > 0. \tag{65}$$
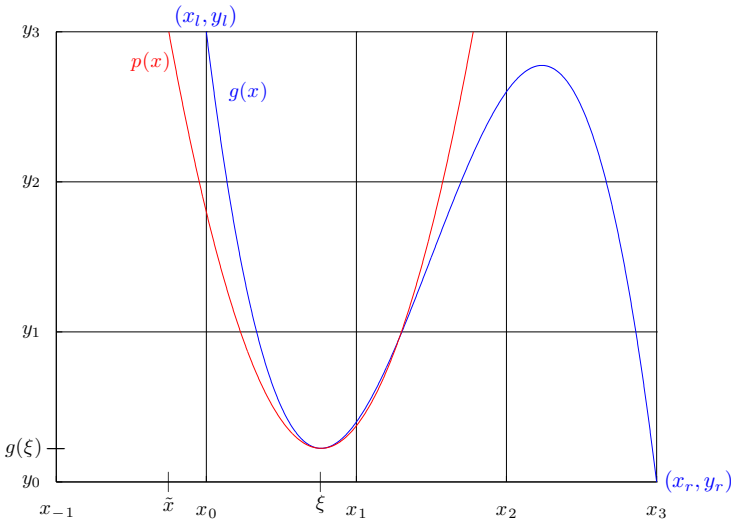
Figure 7. An example in which the interface $g(x)$ enters the 3×3 block of cells B_{ij} at its upper left corner $(x_l, y_l) = (x_0, y_3)$. It then passes through the center cell and leaves B_{ij} at its lower right corner $(x_r, y_r) = (x_3, y_3)$. The function p is the parabolic comparison function used in the proof of case B(1) of Lemma 12.

The first and last of these equations imply that there exists $\zeta \in [x_l, \xi]$ such that

$$f'(\zeta) = g'(\zeta) - p'(\zeta) < 0, \tag{66}$$

and this, together with the middle equation in (65), implies there exists $\eta \in [\zeta, \xi]$ such that

$$f''(\eta) = g''(\eta) - p''(\eta) > 0. \tag{67}$$

In other words,

$$g''(\eta) > p''(\eta) = 2a \quad \text{for some } \eta \in [\zeta, \xi]. \tag{68}$$

Note that $\xi - x_0 \leq 3h/2$ implies that $\xi - \tilde{x} \leq 7h/4$. This inequality, together with $y_3 - g(\xi) > h$, implies

$$g''(\eta) > p''(\eta) = 2a = 2\frac{y_3 - g(\xi)}{(\tilde{x} - \xi)^2} > \frac{32h}{49h^2}.$$

As in the proof of Lemma 11, it follows from (47) that $\kappa^g(\xi) > g''(\xi)/8$; hence

$$\kappa^g(\xi) \geq \frac{g''(\xi)}{8} > \frac{4}{49h} > \frac{4}{52h} > \frac{1}{13h}. \tag{69}$$

Consequently,

$$\kappa_{\max}^g \geq \kappa^g(\xi) > \frac{1}{13h} > \frac{C_h}{h},$$

whereby g fails to satisfy (62), and hence the constraint in (3) as claimed. □

Lemma 13 (Case IV of the Symmetry Lemma). *Let $g \in C^2[x_0, x_3]$ be a function that satisfies the assumptions of Theorem 10. Assume also that the interface g enters the 3×3 block of cells B_{ij} across its left edge at the point $(x_l, y_l) = (x_0, y_l)$, passes through the center cell $C_{ij} = [x_1, x_2] \times [y_1, y_2]$, and exits B_{ij} across its top edge at $(x_r, y_r) = (x_r, y_3)$ with $x_1 < x_r \leq x_3$. Then the interface has at least two column sums in B_{ij} that are either exact or exact to $O(h)$.*

Proof. I will proceed by dividing the problem into two major divisions: (1) the case in which the interface is strictly monotonic and (2) the case in which it is not. The examples in which the center column sum is not exact in any of the four standard orientations of the block B_{ij} — as shown, for example, in Figures 3, 5, 9 and 10 — are in the strictly monotonic category of case IV; the first of these two major divisions.

   In order to make the argument as clear as possible, I have enumerated the proof of case IV into its various subdivisions here.

 (1) The interface g is strictly monotonically increasing.

   (a) The ordinate y_l of the point (x_0, y_l) satisfies $y_0 \leq y_l \leq y_1$. Since g is strictly monotonic, it is invertible. Therefore it can be written as a function $x = g^{-1}(x)$ on the interval $[y_0, y_3]$. Furthermore, since it must pass through the center cell $C_{ij} = [x_1, x_2] \times [y_1, y_2]$ before exiting the block B_{ij} across its top edge, rotation of the block clockwise by 90 degrees will yield an orientation in which the second and third column sums are exact. Thus, this particular case of the lemma is proved.

   (b) The ordinate y_l of the point (x_0, y_l) satisfies $y_1 < y_l < y_2$. There are two subdivisions of this case:

     (i) The abscissa x_r of the point (x_r, y_3) at which the interface exits B_{ij} satisfies $x_2 \leq x_r \leq x_3$. In this case the column sums S_{i-1} and S_i are both exact and the lemma is again proved.

     (ii) The abscissa x_r of the point (x_r, y_3) at which the interface exits B_{ij} is strictly less than right-hand edge $x = x_2$ of the second column. Since the interface is assumed to be a function $y = g(x)$ on the interval $[x_0, x_3]$, and since it must pass through the center cell $C_{ij} = [x_1, x_2] \times [y_1, y_2]$, I have $x_1 < x_r < x_2$. In this case the first column sum S_{i-1} is exact and, since the interface satisfies the constraint $\kappa_{\max} \leq (\sqrt{h})^{-1}$ in (3), the second column sum S_i is exact to $O(h)$. I will prove this latter statement in Theorem 15 below.

(c) The ordinate y_l of the point (x_0, y_l) at which g enters B_{ij} satisfies $y_2 \leq y_l \leq y_3$. Since the interface is strictly monotonically increasing, it cannot enter the center cell $C_{ij} = [x_1, x_2] \times [y_1, y_2]$ if $y_l \geq y_2$. This contradicts the basic assumption that the interface passes through C_{ij}. Therefore this case must be excluded.

(2) The interface is not strictly monotonically increasing.

(a) The abscissa x_r of the point (x_r, y_3) at which the interface exits the block satisfies $x_2 \leq x_r \leq x_3$. In this case the column sums S_{i-1} and S_i are exact and once again the lemma is proved.

(b) The abscissa x_r of the point (x_r, y_3) at which the interface g exits B_{ij} is less than right-hand edge of the second column; that is, $x_r < x_2$. In this case, since g is not strictly monotonic, and since it must pass through the center cell $C_{ij} = [x_1, x_2] \times [y_1, y_2]$, g must have a critical point $(\xi, g(\xi))$ with $y_3 - g(\xi) > h$ which is also a local minimum of g. An example appears in Figure 8. I will now prove that this is inconsistent with

$$\kappa_{\max}^g \leq \frac{C_h}{h}, \tag{70}$$

and hence with the constraint in (3).

Proof of case (2b). Assume that the conditions listed in (2b) above hold and recall that the point $(\xi, g(\xi))$ is a local minimum of g. I form a comparison function p of the form

$$p(x) = a(x - \xi)^2 + g(\xi), \tag{71}$$

where the coefficient a is defined by

$$a = \frac{y_3 - g(\xi)}{(\xi - x_2)^2}. \tag{72}$$

Note that a was chosen so that

$$p(x_2) = y_3 = 3h, \quad p'(\xi) = g'(\xi). \tag{73}$$

Since p is a monotone increasing function for $\xi < x$ and $\xi < x_r$ I must have $g(x_r) > p(x_r)$ as shown, for example, in Figure 8.

Thus, the difference $f(x) = g(x) - p(x)$ between g and p satisfies

$$f(\xi) = g(\xi) - p(\xi) = 0, \quad f'(\xi) = g'(\xi) - p'(\xi) = 0, \quad f(x_r) = g(x_r) - p(x_r) > 0. \tag{74}$$

The first and last of these equations imply there exists $\zeta \in [\xi, x_r]$ such that

$$f'(\zeta) = g'(\zeta) - p'(\zeta) > 0, \tag{75}$$
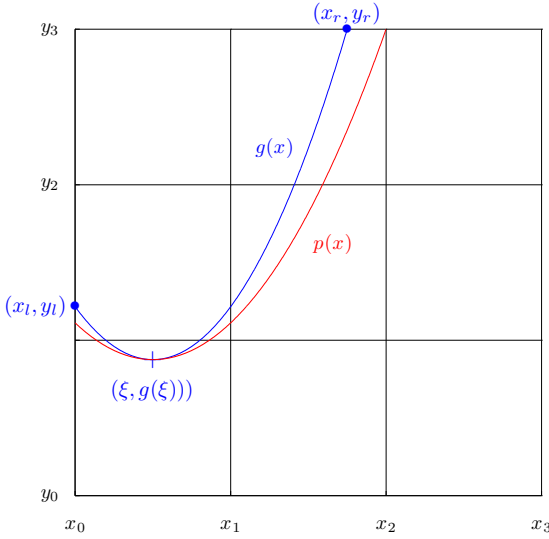
Figure 8. An example in which a nonmonotonic interface $g(x)$ enters the left edge of the 3×3 block B_{ij} at the point $(x_l, y_l) = (x_0, y_l)$ with $y_1 < y_l < y_2$. It then passes through the center cell C_{ij} and leaves B_{ij} at the point $(x_r, y_r) = (x_r, y_3)$ on its top edge with $x_0 < x_r < x_2$. The function $p(x)$ is the parabolic comparison function used in the proof of case (2b) of Lemma 13 to prove that this case cannot occur whenever the interface g satisfies the condition in (70); that is, the first of the two constraints in (3). The presence of a critical point $(\xi, g(\xi)) \in B_{ij}$ is essential to the success of the arguments in which I use a parabolic comparison function p.

and this, together with the middle equation in (74), implies that there exists $\eta \in [\xi, \zeta]$ such that

$$f''(\eta) = g''(\eta) - p''(\eta) > 0. \tag{76}$$

In other words,

$$g''(\eta) > p''(\eta) = 2a \quad \text{for some } \eta \in [\xi, \zeta]. \tag{77}$$

Since $x_2 - \xi < 2h$ and $y_3 - g(\xi) > h$ it follows that

$$g''(\xi) > 2a = 2\frac{(y_3 - g(\xi))}{(x_2 - \xi)^2} = \frac{(2h)}{(x_2 - \xi)^2} > \frac{2h}{4h^2} = \frac{1}{2h}.$$

As in the proof of Lemma 11 I have $\kappa^g(\xi) \geq g''(\xi)/8$ and hence

$$\kappa^g(\xi) \geq \frac{g''(\xi)}{8} > \frac{1}{16h} > \frac{C_h}{h}. \tag{78}$$

Consequently, $\kappa_{\max}^g \geq \kappa^g(\xi) > C_h/h$, whereby g fails to satisfy (70) and hence, the constraint on $\kappa_{\max}$ in (3) as claimed. □

3.2. The comparison circle $\tilde{z}(s)$. All that remains is to prove (ii) from case (1b) in the preceding proof. This is the case in which the center column sum is not exact in each of the four standard orientations of the block B_{ij} as shown in the examples in Figures 3 and 5. The remainder of this section is devoted to proving this result, which is stated explicitly in Theorem 15 below.

Notation. In what follows it will be convenient to translate the coordinate system so that the origin coincides with the point (x_0, y_1). This results in the follow-ing relations, which I will use in several of the proofs below: $(x_0, y_1) = (0, 0)$, $(x_1, y_2) = (h, h)$, and $(x_2, y_3) = (2h, 2h)$, where $x_0, \ldots, x_3$ and $y_0, \ldots, y_3$ are the coordinates of the grid lines as shown, for example, in Figure 9.
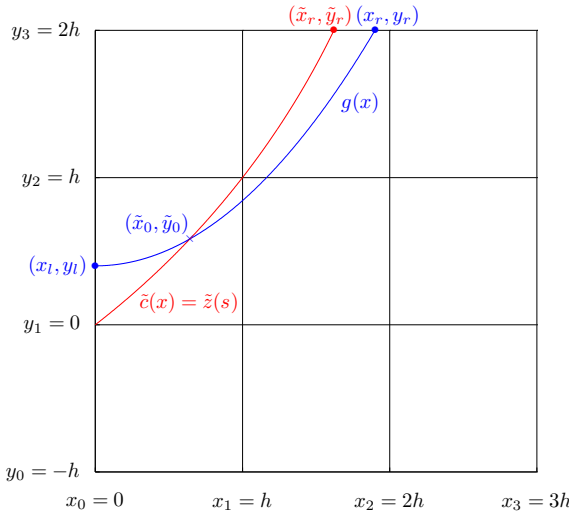
Figure 9. In this figure g is an arbitrary strictly monotonically increasing function that enters the 3×3 block B_{ij} through its left edge at the point (x_l, y_l) with $y_1 \leq y_l < y_2$, passes through the center cell C_{ij}, and exits B_{ij} through the top of its center column S_i at the point (x_r, y_r) with $x_1 < x_r < x_2$. Lemma 16 says that if g satisfies $\kappa_{\max} \leq (\sqrt{h})^{-1}$, the distance $x_2 - x_r$ is $O(h^{3/2})$. In order to prove this, I form a comparison function $\tilde{z}(s)$ which is a circle that has curvature $\tilde{\kappa} = (\sqrt{h})^{-1}$ and passes through (x_0, y_1) and (x_1, y_2). In the circle comparison theorem (Theorem 14) I prove that g must eventually lie below the graph of $\tilde{z}$, thereby implying that $\tilde{x}_r < x_r$. Then, in Lemma 17, I prove that $x_2 - \tilde{x}_r$ is $O(h^{3/2})$.

Now consider the circle $\tilde{\mathbf{z}}(s) = (\tilde{x}(s), \tilde{x}(s))$ defined by

$$\tilde{x}(s) = R \sin\left(\phi_0 + \frac{s}{R}\right) - R \sin\phi_0, \quad \tilde{y}(s) = -R \cos\left(\phi_0 + \frac{s}{R}\right) + R \cos\phi_0, \quad (79)$$

together with the parameters

$$\phi_0 = \frac{\pi}{4} - \sin^{-1}\frac{R}{\sqrt{2}} = \frac{\pi}{4} - \frac{s_1}{2R}, \tag{80}$$

$$s_1 = 2R \sin^{-1}\frac{R}{\sqrt{2}}, \quad s_2 = R \cos^{-1}(\cos\phi_0 - 2R) - R\phi_0. \tag{81}$$

It is relatively straightforward to check the equalities

$$\tilde{\mathbf{z}}(0) = (x_0, y_1) = (0,0), \quad \tilde{\mathbf{z}}(s_1) = (x_1, y_2) = (h, h), \quad \tilde{\mathbf{z}}(s_2) = (\tilde{x}_r, y_3) = (\tilde{x}_r, 2h). \tag{82}$$

Note that the variable $\tilde{x}_r$ in the last of these equations plays the same role with respect to the function $\tilde{\mathbf{z}}(s)$ as the variable x_r plays with respect to the interface $\mathbf{z}(s) = (x, g(x))$. Namely, $\tilde{x}_r$ is the x-coordinate at which the graph of $\tilde{\mathbf{z}}(s)$ exits the top of the 3×3 block B_{ij}. This is illustrated in Figure 9. In what follows I will often use $(x, \tilde{c}(x))$ to denote the graph of $\tilde{\mathbf{z}}(s)$ reparametrized as a function of x just as I use $(x, g(x))$ to denote the graph of the interface $\mathbf{z}(s)$.

3.3. *The circle comparison theorem.*
Suppose that the interface $(x, g(x))$ satisfies $\kappa_{\max} \leq (\sqrt{h})^{-1}$. In the following theorem I prove that once $g(x) < \tilde{c}(x)$ for some $x \in (x_0, x_2)$, then $g(x)$ must remain below $\tilde{c}(x)$ for all $x \in (\tilde{x}_0, \tilde{x}_r)$, where $(\tilde{x}_0, \tilde{y}_0)$ is the point at which g initially crosses $\tilde{c}$ as shown in Figure 9. An immediate consequence of this fact is that $\tilde{x}_r \leq x_r$. Consequently, if $x_r < x_2$, then $\tilde{x}_r \leq x_r < x_2$ and hence $|x_2 - x_r| \leq |x_2 - \tilde{x}_r|$. Since I have constructed the comparison function c so that I can easily show that $|x_2 - \tilde{x}_r|$ is $O(h^{3/2})$, it follows that $|x_2 - x_r|$ is $O(h^{3/2})$. This, together with the fact that $g'(x) \leq \sqrt{3}$ from (46), is sufficient to show that the error in the second column sum associated with g is $O(h)$.

Theorem 14 (The circle comparison theorem). *Assume that $R = \sqrt{h}$ and let $g \in C^2[x_0, x_3]$ be a strictly monotonic function that satisfies*

$$\kappa_{\max} \leq (\sqrt{h})^{-1}. \tag{83}$$

Furthermore, assume that g enters the 3×3 block of cells B_{ij} on its left edge at the point (x_l, y_l) with $y_1 < y_l < y_2$, passes through the center cell C_{ij}, and exits B_{ij} through the top of its center column at the point $(x_r, y_r) = (x_r, y_3)$ with $x_1 < x_r < x_2$. Let $(\tilde{x}_0, \tilde{y}_0)$ denote the first point at which the graph of g crosses the graph of $\tilde{c}$ as shown in, for example, Figure 9. Then

$$g(x) < \tilde{c}(x) \quad \text{for all } x \in (x_0, \tilde{x}_r]. \tag{84}$$

Proof. First note that since $\tilde{c}$ is a circle, the curvature of $\tilde{c}$ is constant: $\kappa^{\tilde{c}} = (\sqrt{h})^{-1}$. Hence, by (83),

$$\kappa^g(x) \leq \kappa^{\tilde{c}}(x) \quad \text{for all } x \in [x_0, \tilde{x}_r].$$

To prove that (84) is true I start by assuming that

$$g(\xi) = \tilde{c}(\xi) \quad \text{for some } \xi \in (x_0, \tilde{x}_r], \tag{85}$$

and then show that this implies that the maximum curvature $\kappa_{\max}$ of g in $(\tilde{x}_0, \tilde{x}_r)$ must exceed $(\sqrt{h})^{-1}$, thereby contradicting (83).

Since $g(x) > \tilde{c}(x)$ for $x_0 < x < \tilde{x}_0$ and $g(x) < \tilde{c}(x)$ for $\tilde{x}_0 < x < \xi$ it follows that

$$g'(\tilde{x}_0) < \tilde{c}'(\tilde{x}_0). \tag{86}$$

However, since by (85) $g(\xi) = \tilde{c}(\xi)$ for some $\xi > \tilde{x}_0$ it must be the case that eventually $g'(x) \geq \tilde{c}'(x)$. Therefore let $x^* \in (\tilde{x}_0, \xi)$ be the first x such that $g'(x^*) = \tilde{c}'(x^*)$. I have

$$g'(x^*) = g'(\tilde{x}_0) + \int_{\tilde{x}_0}^{x^*} g''(x)\, dx = \tilde{c}'(\tilde{x}_0) + \int_{\tilde{x}_0}^{x^*} \tilde{c}''(x)\, dx = \tilde{c}'(x^*),$$

which, by virtue of (86), can only be true if $g''(x) > \tilde{c}''(x)$ on some subinterval of $(\tilde{x}_0, x^*)$. So in particular $g''(\eta) > \tilde{c}''(\eta)$ for some $\eta \in (\tilde{x}_0, x^*)$. Now recall that

(1) g is strictly monotonic and hence $0 < g'(x)$ for all $x \in (x_0, \tilde{x}_r]$.

(2) $0 < g'(x) < \tilde{c}'(x)$ for all $x \in (\tilde{x}_0, x^*)$.

(3) $\kappa^g(x) = g''(x)(1 + g'(x)^2)^{-3/2}$ for all x.

Items (1)–(3) imply that

$$\kappa^g(\eta) = \frac{g''(\eta)}{(\sqrt{1 + g'(\eta)^2})^3} > \frac{\tilde{c}''(\eta)}{(\sqrt{1 + \tilde{c}'(\eta)^2})^3} = \kappa^{\tilde{c}}(\eta) = \frac{1}{\sqrt{h}},$$

which contradicts (83) as claimed. $\square$

3.4. *The column sum S_i is exact to $O(h)$.*

Theorem 15 (The column sum S_i is exact to $O(h)$). *Assume that the interface $g \in C^2[x_0, x_3]$ and that g is a strictly monotonically increasing function that satisfies*

$$\kappa_{\max} \leq (\sqrt{h})^{-1}. \tag{87}$$

Furthermore, assume that the g enters the 3×3 block of cells B_{ij} on its left edge at the point (x_l, y_l) with $y_1 \leq y_l \leq y_3$, passes through the center cell $C_{i,j} = [x_1, x_2] \times [y_1, y_2]$, and exits B_{ij} through the top of its center column at the point $(x_r, y_r) = (x_r, y_3)$ with $x_1 < x_r < x_2$ as shown, for example, in Figure 10. Then the
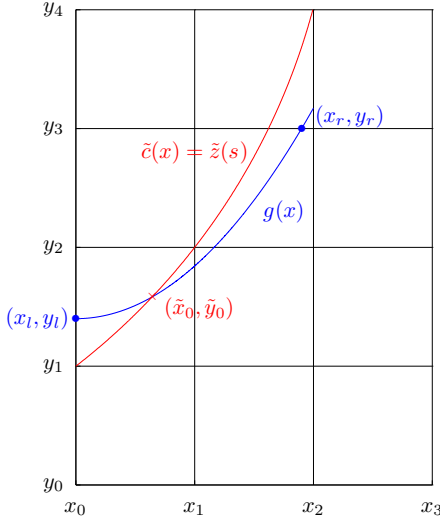
Figure 10. To see the error between the center column sum S_i and the exact volume (area) under the interface $y = g(x)$, I have plotted the row of cells that lie above the standard 3×3 block of cells $B_{i,j}$ centered on the cell $C_{i,j} = [x_1, x_2] \times [y_1, y_2]$ in which the approximation to the interface g will be constructed. I have also plotted the comparison circle $\tilde{c}(x)$ which, in Theorem 14, I prove provides an upper bound on $g(x)$ for all $x \in [\tilde{x}_0, x_2]$ where $(\tilde{x}_0, \tilde{y}_0)$ is the point at which the interface g intersects comparison circle $\tilde{c}$.

error between the column sum S_i and the normalized integral of g over the second column is $O(h)$:

$$\left| S_i - h^{-2} \int_{x_1}^{x_2} (g(x) - y_0) \, dx \right| \leq C_S h, \tag{88}$$

where

$$C_S = 8\sqrt{3}(2\sqrt{2} - 1)^2. \tag{89}$$

Proof. As one can see from the example shown in Figure 10, the error between the column sum S_i and the exact normalized volume (area) under the interface $y = g(x)$ in the center column is

$$h^{-2} \int_{x_1}^{x_2} (g(x) - y_0) \, dx - S_i = h^{-2} \int_{x_r}^{x_2} (g(x) - y_3) \, dx,$$

since

$$S_i = h^{-2} \int_{x_1}^{x_2} (\min\{g(x), y_3\} - y_0) \, dx,$$

and, by assumption, $\min_{[x_0, x_r]} g(x) \geq y_l \geq y_1$. Thus, it suffices to show that

$$\left| \int_{x_r}^{x2} (g(x) - y_3) dx \right| \leq C_S h^3. \tag{90}$$

In other words, I need to show that the volume in the region below the interface $y = g(x)$ that lies in the cell $C_{2,4}$ is $O(h^3)$.

By (46) in I have $|g'(x)| \leq \sqrt{3}$. This implies

$$\left| \int_{x_r}^{x2} (g(x) - y_3) dx \right| \leq \left| \int_{x_r}^{x2} l(x) dx \right|, \tag{91}$$

where $l(x)$ is the line with slope $\sqrt{3}$ that passes through the point x_r. The region of integration on the right side of (91) is a right triangle with corners (x_r, y_3), (x_2, y_3), and $(x_2, y_3 + \sqrt{3}(x_2 - x_r))$ and the integral is the area of this triangle, namely, $\sqrt{3}(x_2 - x_r)^2/2$. Thus I have

$$\left| \int_{x_r}^{x2} (g(x) - y_3) dx \right| \leq \left| \int_{x_r}^{x2} l(x) dx \right| \leq \frac{\sqrt{3}}{2}(x_2 - x_r)^2 \leq \frac{\sqrt{3}}{2}\tilde{C}^2 h^3, \tag{92}$$

where the bound $(x_2 - x_r)^2 \leq \tilde{C}^2 h^3$ between the second to last and last terms in (92) follows from the inequality (93) immediately below. Equation (92) implies (90). Equation (88) — and hence the theorem — follows immediately. □

Lemma 16 ($x_2 - x_r$ is $O(h^{3/2})$). *Let $g \in C^2[x_0, x_3]$ be a function that satisfies the assumptions stated in Theorem 14. Then*

$$x_2 - x_r \leq \tilde{C} h^{3/2}, \tag{93}$$

where

$$\tilde{C} = 4(2\sqrt{2} - 1). \tag{94}$$

Proof. By the circle comparison theorem (Theorem 14) there exists a point $\tilde{x}_0 \in [x_0, x_r)$ such that

$$g(x) \leq \tilde{c}(x) \quad \text{for all } x \in [\tilde{x}_0, x_r].$$

This implies that $\tilde{x}_r \leq x_r$. Since by assumption $x_r < x_2$, Equation (93) follows immediately from Equation (95) in Lemma 17 below. □

Lemma 17 ($x_2 - \tilde{x}_r$ is $O(h^{3/2})$). *Let $R = \sqrt{h}$ and let $\tilde{x}_r$ be defined as in (82) above. Then*

$$x_2 - \tilde{x}_r \leq \tilde{C} h^{3/2}, \tag{95}$$

where $\tilde{C}$ is defined in (94).

Proof. Since the coordinate system has been arranged so that the origin is at the point (x_0, y_1) and hence $x_2 = 2h = y_3$ (for example, see Figure 9), I have

$$x_2 = \tilde{y}_r = \tilde{y}(s_2).$$

Thus

$$
\begin{aligned}
x_2 - \tilde{x}_r &= \tilde{y}(s_2) - \tilde{x}(s_2) \\
&= R\{(\cos\phi_0 - \cos(\phi_0 + s_2/R)) - (-\sin\phi_0 + \sin(\phi_0 + s_2/R))\},
\end{aligned}
\tag{96}
$$

and since $R = \sqrt{h}$, it suffices to show that the quantity inside the curly braces in (96) is $O(R^2) = O(h)$. I can rewrite (96) as

$$
x_2 - \tilde{x}_r = R\{(\cos\phi_0 + \sin\phi_0) - (\cos(\phi_0 + \theta) + \sin(\phi_0 + \theta))\},
\tag{97}
$$

where $\theta = s_2/R$. Consider the quantity A defined by dividing (97) by R:

$$
A = \{(\cos\phi_0 + \sin\phi_0) - (\cos(\phi_0 + \theta) + \sin(\phi_0 + \theta))\}.
\tag{98}
$$

Now expand $\cos(\phi_0 + \theta)$ and $\sin(\phi_0 + \theta)$ in a Taylor series about $\cos\phi_0$ and $\sin\phi_0$ to obtain

$$
\begin{aligned}
A &= (\cos\phi_0 + \sin\phi_0) - \big(\cos(\phi_0 + \theta) + \sin(\phi_0 + \theta)\big) \\
&= -(\cos\phi_0 - \sin\phi_0)\theta + (\cos\phi_0 + \sin\phi_0)\frac{\theta^2}{2!} + (\cos\phi_0 - \sin\phi_0)\frac{\theta^3}{3!} \\
&\quad -(\cos\phi_0 + \sin\phi_0)\frac{\theta^4}{4!} - (\cos\phi_0 - \sin\phi_0)\frac{\theta^5}{5!} + (\cos\phi_0 + \sin\phi_0)\frac{\theta^6}{6!} + \cdots.
\end{aligned}
$$

After some manipulation one obtains

$$
\begin{aligned}
A = &-\left((\cos\phi_0 - \sin\phi_0) - (\cos\phi_0 + \sin\phi_0)\frac{\theta}{2}\right)\theta \\
&+\left((\cos\phi_0 - \sin\phi_0) - (\cos\phi_0 + \sin\phi_0)\frac{\theta}{4}\right)\frac{\theta^3}{3!} \\
&-\left((\cos\phi_0 - \sin\phi_0) - (\cos\phi_0 + \sin\phi_0)\frac{\theta}{6}\right)\frac{\theta^5}{5!} + \cdots.
\end{aligned}
\tag{99}
$$

The first term in this series is $O(R^2) = O(h)$. To see this note that by Lemma 19 below $\cos\phi_0 - \sin\phi_0 = R$ and $\cos\phi_0 + \sin\phi_0 = \sqrt{2 - R^2}$ so that the series for A in (99) becomes

$$
A = -\left(R - \frac{\theta}{2}\sqrt{2 - R^2}\right)\theta + \left(R - \frac{\theta}{4}\sqrt{2 - R^2}\right)\frac{\theta^3}{3!} - \left(R - \frac{\theta}{6}\sqrt{2 - R^2}\right)\frac{\theta^5}{5!} + \cdots.
\tag{100}
$$

The first term is positive, because $R = \sqrt{h}$, $\theta = s_2/R$, and $s_2 \geq h$ (see (102) below). Thus,

$$
\left(\frac{\theta}{2}\sqrt{2 - R^2} - R\right)\theta \geq \left(\frac{h}{R}\sqrt{2 - R^2} - R\right)\frac{h}{R} \geq \left(\sqrt{2 - R^2} - 1\right)R^2 > 0,
$$

for all $0 < h \leq 1$, and hence all $0 < R \leq 1$. Similarly, since $s_2 \leq 4h$ (see Lemma 18 again), it follows that

$$\left(\frac{\theta}{2}\sqrt{2-R^2}-R\right)\theta \leq \left(2R\sqrt{2-R^2}-R\right)4R = 4\left(2\sqrt{2-R^2}-1\right)R^2, \quad (101)$$

for all $0 < h \leq 1$, or equivalently all $0 < R \leq 1$. Combining equations (97), (98), (100), and (101) yields

$$x_2 - \tilde{x}_r \leq 4(2\sqrt{2-R^2}-1)R^3 + O(R^5) \leq 4(2\sqrt{2}-1)R^3 + O(R^5).$$

It is possible to show — for example by plotting it with MATLAB — that the co-efficient $(R - \theta\sqrt{2-R^2})/4$ of the second term in the expansion of A in terms of R in (100) is negative for $0 < h \leq 1$ and that furthermore, the tail of the series is bounded by this term. Equation (95) follows immediately. $\qquad \square$

Lemma 18 ($s_2 = O(h)$). *Assume that $h \leq 1$ and let s_2 be defined as in* (81). *Then*

$$h \leq s_2 \leq 4h. \qquad (102)$$

Proof. First, note that I am only interested in functions g that exit the 3×3 block of cells at the point (x_r, y_3) when $x_r < x_2$ as shown for example in Figure 3. For otherwise the first and second column sums would be exact and I would be done.
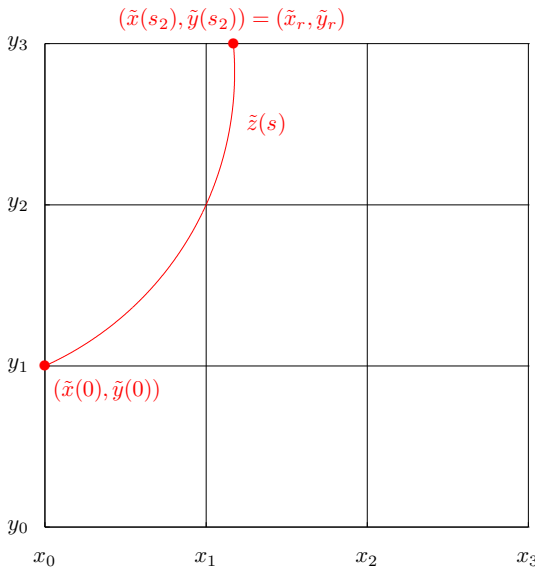
Figure 11. In this figure $h = \frac{1}{4}$ and hence the comparison circle $\tilde{\mathbf{z}}(s)$ has radius $R = \sqrt{h} = 2h$.

Since a consequence of Theorem 14 is that $\tilde{x}_r = \tilde{x}(s_2) \le x_r$, it follows that I am only interested in values of $R = \sqrt{h}$ and s_2 such that $\tilde{x}_r < x_2$.

To obtain the lower bound on s_2 in (102) note that s_2 is an arc of the circle $\tilde{z}$ and that when $h = 1$ the radius of $\tilde{z}$ is $R = \sqrt{h} = h$. In this case the point $(\tilde{x}_r, \tilde{y}_r) = (x_0, y_3)$ and hence $\tilde{x}_r = x_0$. Since this is half the circumference of the circle with center (x_0, y_2) and radius h, $s_2 = \pi$ when $h = 1$. Since s_2 will always be greater than the length of the chord connecting the points (x_0, y_1) and $(\tilde{x}_r, \tilde{y}_r)$ and since this particular chord is the diameter of $\tilde{z}$ all other chords of $\tilde{z}$ will be smaller. In particular, since the radius of $\tilde{z}$ $R = \sqrt{h} \to 0$ as $h \to 0$, all chords connecting (x_0, y_1) and $(\tilde{x}_r, \tilde{y}_r)$ will be smaller than this one. The lower bound on s_2 in (102) follows immediately.

In order to write s_2 in the form $s_2 = Ch$ where C is a constant independent of h note that since $h \le 1$ and $\tilde{x}(s_2) < x_2$, the arc of the circle that connects the points $(\tilde{x}(0), \tilde{y}(0))$ and $(\tilde{x}(s_2), \tilde{y}(s_2))$ always lies entirely within the triangle with vertices (x_0, y_1), (x_2, y_1) and (x_2, y_3), as shown in Figure 11, for example. Hence, the arc length s_2 will always be bounded above by the sum of the lengths of the two perpendicular sides of this right triangle; namely,

$$s_2 < 4h.$$

This is the upper bound on s_2 in (102). $\qquad\qquad\square$

In order to prove that $x_2 - \tilde{x}_r = O(h^{3/2})$ in Lemma 17, I expanded $x_2 - \tilde{x}_r$ in a Taylor series about the point ϕ_0. As we saw in Lemma 17 the coefficient of the first nonzero term in this expansion is $\cos\phi_0 - \sin\phi_0$. Hence, the fact that $\cos\phi_0 - \sin\phi_0 = R$ is a crucial part of the proof that $|x_2 - \tilde{x}_r| = O(h^{3/2})$. The purpose of the following lemma is to prove this fact and also to establish the value of $\cos\phi_0 + \sin\phi_0$.

Lemma 19 ($\cos\phi_0 - \sin\phi_0 = R$). *Let ϕ_0 be defined as in* (80):

$$\phi_0 = \frac{\pi}{4} - \sin^{-1}\frac{R}{\sqrt{2}}.$$

Then

$$\cos\phi_0 - \sin\phi_0 = R, \quad \cos\phi_0 + \sin\phi_0 = \sqrt{2 - R^2}. \qquad (103)$$

Proof. Define θ by $\sin\theta = R/\sqrt{2}$, so that

$$\phi_0 = \frac{\pi}{4} - \sin^{-1}\frac{R}{\sqrt{2}} = \frac{\pi}{4} - \theta.$$

The first equation in (103) follows from writing ϕ_0 as $\pi/4 - \theta$ and applying the trigonometric identities for the sine and cosine of the difference of two angles:

$$\cos\phi_0 - \sin\phi_0 = \sqrt{2}\sin\theta = R.$$

To prove the second equality in (103) I again use the trigonometric identities for the sine and cosine of the difference of two angles, together with the trigonometric identity $\cos(\arcsin x) = \sqrt{1 - x^2}$, to obtain

$$\cos \phi_0 + \sin \phi_0 = \sqrt{2} \cos \theta = \sqrt{2} \cos\left(\sin^{-1} \frac{R}{\sqrt{2}}\right) = \sqrt{2 - R^2}. \qquad \square$$

4. Second-order accuracy in the max norm

In this section I will assume the coordinate system has been arranged so that the bottom edge of the 3×3 block of cells B_{ij} lies along the line $y = 0$ and that the vertical line $x = x_c$ which passes through the center of the center cell is $x = 0$ as shown in Figure 12. In particular, note that the origin is at the center of the bottom edge of the 3×3 block and the center of C_{ij} is $(0, 3h/2)$ as shown in the figure.

I will also denote the interval that forms the bottom of the 3×3 block B_{ij} by I, and the intervals $[x_{i-2}, x_{i-1}]$, $[x_{i-1}, x_i]$ and $[x_i, x_{i+1}]$ that are associated with the three columns of B_{ij} by $I_{i+\alpha}$ for $\alpha = -1, 0, 1$. Thus, $I = [-3h/2, 3h/2]$ and

$$I_{i+\alpha} \equiv \begin{cases} [-3h/2, -h/2] & \text{if } \alpha = -1, \\ [-h/2, h/2] & \text{if } \alpha = 0, \\ [h/2, 3h/2] & \text{if } \alpha = 1. \end{cases}$$
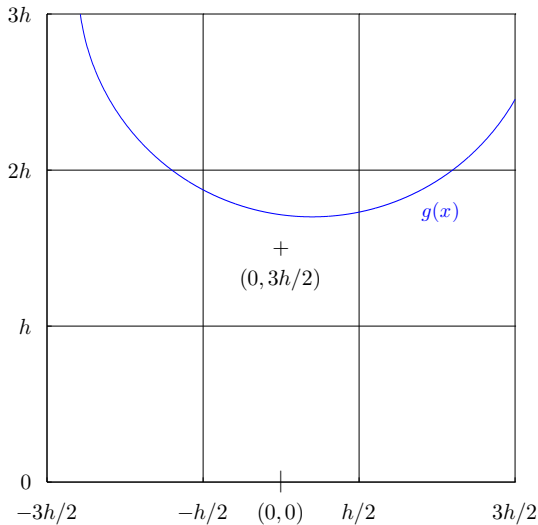
Figure 12. In this section I will work with the coordinate system shown here. The origin is at the center of the bottom of the 3×3 block B_{ij} so that the center of the center cell C_{ij} is $(0, 3h/2)$ as shown in the figure. This latter point corresponds to the point labeled (x_c, y_c) in some of the other figures.

Given an arbitrary integrable function $g(x)$ on the interval $I = [-3h/2, 3h/2]$, let $\Lambda_{i,j}(g)$ denote the volume fraction due to g in the center cell

$$\Lambda_{i,j}(g) = h^{-2} \int_{I_i} \theta_j(g(x)) \, dx. \tag{104}$$

where $\theta_j(g)$ is defined by

$$\theta_j(g) \equiv (g(x) - (j-1)h)_+ - (g(x) - jh)_+ \tag{105}$$

and

$$x_+ = \begin{cases} x & \text{if } x > 0, \\ 0 & \text{if } x \le 0, \end{cases} \tag{106}$$

is the ramp function. I will denote the volume fractions in the other cells similarly; that is, I will use $\Lambda_{i',j'}(g)$ for $i' = i-1, i, i+1$ and $j' = j-1, j, j+1$ to denote the volume fraction in the (i', j')-th cell. When the function g under consideration is apparent, I will simply write $\Lambda_{i',j'}$ or equivalently $\Lambda_{i+\alpha,j+\beta}$ for some $\alpha, \beta = -1, 0, 1$.

In the following lemma I make the implicit assumption that the 3×3 block of cells B_{ij} has been arranged so that the volume fraction $\Lambda_{i,j}(g)$ is the volume (area) of *dark fluid* in the center cell. In other words, if one assumes that the block B_{ij} has been rotated so that the interface $\mathbf{z}$ can be represented as a function $g(x)$ on the interval $I = [-3h/2, 3h/2]$, then there are two possibilities:

(1) $\Lambda_{i,j}(g) = h^{-2} \int_{I_i} \theta_j(g) \, dx$ is the volume of dark fluid in C_{ij},

(2) $\Lambda_{i,j}(g) = h^{-2} \int_{I_i} \theta_j(g) \, dx$ is the volume of light fluid in C_{ij}.

In the event that (2) holds, one can reflect the 3×3 block B_{ij} about the line $y = y_c$, where $y_c = (y_j + y_{j+1})/2$ is the line that divides the block $B_{i,j}$ in half horizontally, to ensure that case (1) holds. This is necessary because when I write the piecewise linear approximation $\tilde{g}_{i,j}(x) = m_{i,j}x + b_{i,j}$ to $g(x)$ in $C_{i,j}$ I am implicitly assuming that

$$\Lambda_{i,j}(\tilde{g}_{i,j}) = h^{-2} \int_{I_i} \theta_j(\tilde{g}_{i,j}(x)) \, dx$$

is the volume of dark fluid in $C_{i,j}$. It is necessary to be consistent about which fluid is represented by the volume fraction $\Lambda_{i,j}$ in order to prove the following lemma.

Lemma 20 (Equal volume fractions ensure that $\tilde{g}$ intersects g in the center cell $C_{i,j}$). *Let $g(x)$ be a continuous function on the interval $I_i \equiv [-h/2, h/2]$ and assume that a portion of the interface $g(x)$ passes through the center cell*

$$C_{i,j} = [-h/2, h/2] \times [h, 2h].$$

Furthermore, assume that the 3×3 block of cells B_{ij} centered on $C_{i,j}$ has been arranged so that

$$\Lambda_{i,j}(g) = h^{-2} \int_{I_i} \theta_j(g(x)) \, dx \tag{107}$$

is the (nonzero) volume fraction of dark fluid in $C_{i,j}$. Let

$$\tilde{g}(x) = mx + b \tag{108}$$

be a piecewise linear approximation to g that passes through the center cell $C_{i,j}$ and assume that g and $\tilde{g}$ have the same volume fraction

$$0 < \Lambda_{i,j}(g) = \Lambda_{i,j}(\tilde{g}) < 1$$

in C_{ij}. Then there exists a point $x^* \in I_i = [-h/2, h/2]$ such that

$$g(x^*) = \tilde{g}(x^*).$$

Proof. Consider

$$h^{-2} \int_{I_i} \left[\theta_j(g(x)) - \theta_j(\tilde{g}(x)) \right] dx = \Lambda_{i,j}(g) - \Lambda_{i,j}(\tilde{g}) = 0,$$

and note that $\theta_j(g)$ defined in (105) is a strictly monotonically increasing function of $g(x)$:

$$g(x) < \tilde{g}(x) \Rightarrow \theta_j(g(x)) < \theta_j(\tilde{g}(x)).$$

Therefore, in order for $\Lambda_{i,j}(g) = \Lambda_{i,j}(\tilde{g})$ to hold, there are two possibilities. The first is that $g(x) = \tilde{g}(x)$ for all $x \in I_i$, in which case the theorem is true and x^* is any point in I_i.

The second possibility is that there exists a point $x_- \in I_i$ with $g(x_-) < \tilde{g}(x_-)$ and there also exists a point $x_+ \in I_i$ where $g(x_+) > \tilde{g}(x_+)$. Thus, since both $g(x)$ and $\tilde{g}(x)$ are continuous, there must be a point x^* between x_- and x_+ where $g(x^*) = \tilde{g}(x^*)$. To see this, consider the function $f(x) = g(x) - \tilde{g}(x)$. The function f is continuous and furthermore,

$$f(x_+) = g(x_+) - \tilde{g}(x_+) > 0, \quad f(x_-) = g(x_-) - \tilde{g}(x_-) < 0.$$

Hence, if $x_- < x_+$, then there must exist an $x^* \in (x_-, x_+) \subset I_i$ (or, if $x_+ < x_-$, then $x^* \in (x_+, x_-) \subset I_i$) such that $f(x^*) = 0$, or equivalently, $g(x^*) = \tilde{g}(x^*)$, as claimed. $\qquad \square$

An immediate consequence of this lemma is that the piecewise constant volume-of-fluid interface reconstruction algorithm as defined below must be first-order accurate. The details are as follows.

Definition 21. The *piecewise constant VOF interface reconstruction algorithm* is defined by

$$\tilde{g}(x) = y_{j-1} + h\Lambda_{i,j}(g) \quad \text{for all } x \in I_i = [x_{i-1}, x_i], \tag{109}$$

where, as usual, I have assumed that the 3×3 block B_{ij} centered about the cell C_{ij} in which I want to reconstruct the interface has been rotated so that the interface can be written as a single valued function $g(x)$ on the interval $I = [-3h/2, 3h/2]$ and

$$\Lambda_{i,j}(g) = h^{-2} \int_{I_i} \theta_j(g)\,dx$$

is the volume of dark fluid in C_{ij}.

Corollary 22 (The piecewise constant VOF interface reconstruction algorithm is first-order). *Suppose that the interface passes through a portion of the cell $C_{i,j}$ and that it can be represented as a C^2 function on the interval $I = [-3h/2, 3h/2]$. Then the piecewise constant interface reconstruction algorithm defined in* (109) *produces a first-order accurate approximation $\tilde{g}$ to the exact interface g in $C_{i,j}$:*

$$|g(x) - \tilde{g}(x)| \le C_P h \quad \text{for all } x \in I_i = [-h/2, h/2],$$

where $C_P = \sqrt{3}$.

Proof. By assumption the interface g is continuous and passes through the center cell C_{ij}. Furthermore, the piecewise constant interface reconstruction algorithm defined in (109) is a member of the class of piecewise linear approximations to g. Therefore, Lemma 20 applies, and hence there exists a point $x^* \in I_i$ such that $y_{j-1} \le g(x^*) \le y_j$ and

$$g(x^*) = \tilde{g}(x^*).$$

The assumption[10] that $g \in C^2[I]$ allows me to apply Theorem 6 to obtain (see Equation (46))

$$|g'(x)| \le \sqrt{3} \quad \text{for all } x \in [-h/2, h/2]. \tag{110}$$

Thus, applying the Taylor remainder theorem [29] to $g(x)$, I find that for all $x \in [-h/2, h/2]$

$$|g(x) - \tilde{g}(x)| = |g(x^*) + g'(\xi)(x - x^*) - \tilde{g}(x^*)| \le |g'(\xi)h| \le \sqrt{3}h,$$

since $\xi = \xi(x)$ is some number between x and x^* (that is, $\xi \in [-h/2, h/2]$) and hence, (110) applies. $\qquad\square$

---

[10]Actually, I only need the interface g to be one times continuously differentiable on I_i; that is, $g \in C^1[I_i]$. I have assumed $g \in C^2[I]$ here so that I will not have to prove a special version of Theorem 6 in order to obtain the bound in (46) on $g'(x)$.

Theorem 23 (The approximation to g' is first-order accurate). *Assume that the interface $g \in C^2[I]$ where $I = [-3h/2, 3h/2]$ and that at least two distinct column sums $S_{i+\alpha}$ and $S_{i+\beta}$ with $\alpha, \beta = 1, 0, -1$ and $\alpha \neq \beta$ are exact to $O(h)$:*

$$\left| S_{i+\alpha} - h^{-2} \int_{I_{i+\alpha}} g(x)\, dx \right| \leq C_S h, \tag{111}$$

$$\left| S_{i+\beta} - h^{-2} \int_{I_{i+\beta}} g(x)\, dx \right| \leq C_S h, \tag{112}$$

where

$$C_S = 8\sqrt{3}(2\sqrt{2} - 1)^2 \tag{113}$$

is the constant obtained in [Theorem 15]. Then the slope defined by

$$m = \frac{S_{i+\alpha} - S_{i+\beta}}{\alpha - \beta} \quad \text{for } \alpha, \beta = 1, 0, -1 \text{ with } \alpha \neq \beta$$

of the piecewise linear approximation $\tilde{g}(x) = mx + b$ to the exact interface g satisfies

$$|m - g'(0)| \leq \left(\tfrac{26}{3} \kappa_{\max} + C_S \right) h. \tag{114}$$

Proof. Note that during the course of proving [Theorem 10], I have shown that the only column sum that may not be exact is the middle one, S_i; for example, see the list in the proof of the [Symmetry Lemma]. Therefore, I may assume that

$$S_{i+\alpha} = h^{-2} \int_{I_{i+\alpha}} g(x)\, dx \quad \text{if } \alpha = 1 \text{ or } -1. \tag{115}$$

Now note that the inequality in [(88)] can be rewritten in the following way. If [(88)] holds for the i-th column sum S_i, then there exists $\epsilon_i > 0$ with $|\epsilon_i| \leq C_S h$ such that

$$h^{-2} \int_{I_i} g(x)\, dx = S_i + \epsilon_i \quad \text{if } \alpha = 0. \tag{116}$$

In other words, if the column sum S_i is not exact, then ϵ_i is the area of the region bounded by the horizontal line $y = y_3$, the vertical line $x = x_2$, and the graph of the interface $y = g(x)$ as shown in [Figure 10]. Otherwise, the column sum S_i is exact and $\epsilon_i = 0$.

By the Taylor remainder theorem

$$g(x) = g(0) + g'(0)x + \tfrac{1}{2} g''(\xi) x^2, \tag{117}$$

for some $\xi \in (-x, x)$.[11] Applying (117) to g and performing the integration in equations (115) and (116) for each $\alpha = -1, 0, 1$ yields

$$S_{i-1} = g(0)h^{-1} - g'(0) + \tfrac{13}{24}g''(\xi_{-1})h, \tag{118}$$

$$S_i = g(0)h^{-1} + \tfrac{1}{24}g''(\xi_0)h - \epsilon_i, \tag{119}$$

$$S_{i+1} = g(0)h^{-1} + g'(0) + \tfrac{13}{24}g''(\xi_1)h, \tag{120}$$

where the term with $g'(0)$ has dropped out of the expression for S_i, since $g'(0)x$ is an odd function of x and the interval $I_i = [-h/2, h/2]$ is centered about $x = 0$.

Subtracting the expression in (118) from the expression in (120) and dividing by 2 yields the centered difference approximation to the derivative $g'(0)$ plus error terms:

$$\frac{S_{i+1} - S_{i-1}}{2} = g'(0) + \tfrac{13}{24}\big(g''(\xi_1) + g''(\xi_{-1})\big)h. \tag{121}$$

Rearranging the terms in (121) and using (47) yields

$$\left|\frac{S_{i+1} - S_{i-1}}{2} - g'(0)\right| = \left|\tfrac{13}{24}\big(g''(\xi_1) + g''(\xi_{-1})\big)h\right| \le \tfrac{26}{3}\kappa_{\max}h \le \big(\tfrac{26}{3}\kappa_{\max} + C_S\big)h.$$

Similarly, subtracting S_{i-1} from S_i and S_i from S_{i+1} yield the two one-sided difference approximations to $g'(0)$,

$$|(S_i - S_{i-1}) - g'(0)| \le \big(\tfrac{14}{3}\kappa_{\max} + C_S\big)h,$$

$$|(S_{i+1} - S_i) - g'(0)| \le \big(\tfrac{14}{3}\kappa_{\max} + C_S\big)h.$$

The inequality in (114) follows immediately. $\qquad\square$

The following theorem is the main result of this paper.

Theorem 24. *Assume the interface $g \in C^2[I]$ where $I = [-3h/2, 3h/2]$ and that at least two of the column sums $S_{i+\alpha}$ and $S_{i+\beta}$ for $\alpha, \beta = 1, 0, -1$ with $\alpha \ne \beta$ are exact to $O(h)$. Let*

$$\tilde{g}(x) = mx + b$$

be a piecewise linear approximation to $g(x)$ in $I_i = [-h/2, h/2]$ with

$$m = \frac{S_{i+\alpha} - S_{i+\beta}}{\alpha - \beta}, \tag{122}$$

and assume that $g(x)$ and $\tilde{g}(x)$ have the same volume fraction in the center cell:

$$\Lambda_{i,j}(g) = \Lambda_{i,j}(\tilde{g}).$$

---

[11]Technically speaking, if $x > 0$, then $\xi \in (0, x)$, while if $x < 0$, then $\xi \in (x, 0)$. My intention is for the notation $\xi \in (-x, x)$ to cover both cases.

Then $\tilde{g}(x)$ is a second-order accurate approximation to $g(x)$ in I_i:

$$|g(x) - \tilde{g}(x)| \le \left(\tfrac{50}{3}\kappa_{\max} + C_S\right)h^2 \quad \text{for all } x \in I_i = [-h/2, h/2]$$

where

$$C_S = 8\sqrt{3}(2\sqrt{2} - 1)^2. \tag{123}$$

Proof. By Lemma 20 I know that there exists $x^* \in I_i = [-h/2, h/2]$ such that $g(x^*) = \tilde{g}(x^*)$. Let $x \in I_i$ be arbitrary, but fixed. By the Taylor remainder theorem I know that there exists $\xi = \xi(x) \in I_i$ such that

$$g(x) = g(x^*) + g'(x^*)(x - x^*) + \tfrac{1}{2}g''(\xi)(x - x^*)^2.$$

Hence,

$$
\begin{aligned}
|g(x) - \tilde{g}(x)| &= \left| g(x^*) + g'(x^*)(x - x^*) + \tfrac{1}{2}g''(\xi)(x - x^*)^2 - \tilde{g}(x^*) - m(x - x^*) \right| \\
&\le |g'(x^*) - m||x - x^*| + \tfrac{1}{2}|g''(\xi)|(x - x^*)^2 \\
&\le |g'(x^*) - m|h + 4\kappa_{\max}h^2,
\end{aligned}
$$

where I have used (47) to bound $g''(\xi)$ and the fact that $x, x^* \in I_i = [-h/2, h/2]$ to obtain $|x - x^*| \le h$. In order to bound $\left|g'(x^*) - m\right|$ I rewrite this expression as:

$$|g'(x^*) - m| = |g'(x^*) - g'(0)| + |g'(0) - m|. \tag{124}$$

In order to bound the first term on the right side of (124) I expand $g'(x^*)$ in a Taylor series about $x = 0$ and use the Taylor remainder theorem to obtain

$$g'(x^*) = g'(0) + g''(\zeta)(x^* - 0),$$

for some $\zeta \in I_i$. From (47) and, since $x^* \in I_i = [-h/2, h/2]$ implies $|x^*| \le h/2$, I have

$$|g'(x^*) - g'(0)| \le |g''(\zeta)||x^*| \le 4\kappa_{\max}h. \tag{125}$$

Finally, using the bound on $|g'(0) - m|$ in (114), I have

$$
\begin{aligned}
|g(x) - \tilde{g}(x)| &\le (|g'(x^*) - g'(0)| + |g'(0) - m|)h + 4\kappa_{\max}h^2 \\
&\le \left(8 + \tfrac{26}{3}\right)\kappa_{\max}h^2 + C_Sh^2 = \left(\tfrac{50}{3}\kappa_{\max} + C_S\right)h^2,
\end{aligned}
$$

as claimed. $\qquad\qquad\qquad\qquad\qquad\qquad\qquad\qquad\qquad\qquad\qquad\qquad\square$

5. Conclusions

Given any C^2 curve $\mathbf{z}(s)$ in $\mathbb{R}^2$ overlaid with a computational grid consisting of square cells, each with (nondimensional) side h, I have proven that for each cell C_{ij} that contains a portion of the curve $\mathbf{z}(s)$ there exist at least two columns or two rows in the 3×3 block of cells B_{ij} centered on the cell C_{ij} whose divided

difference is a first-order accurate approximation m_{ij} to the slope of the curve $\mathbf{z}(s)$ in the center cell C_{ij}. This approximation to the slope of $\mathbf{z}$ in C_{ij}, together with the knowledge of the exact volume fraction Λ_{ij} in C_{ij}, is sufficient to construct a line segment $\tilde{g}_{ij}(x)$ that is an $O(h^2)$ approximation to the curve $\mathbf{z}(s) = (x(s), g(x(s))$ it in the max norm in that cell:

$$|g(x) - \tilde{g}_{ij}(x)| \leq C(\kappa_{\max})h^2 \quad \text{for all } x \in [x_i, x_{i+1}]. \tag{126}$$

Here $\kappa_{\max}$ is the maximum curvature of the interface $\mathbf{z}$ in the 3×3 block of cells B_{ij} centered on the cell C_{ij}, $C(\kappa_{\max})$ is a constant that depends on $\kappa_{\max}$ but is independent of h, and x_i, x_{i+1} denote the left and right edges, respectively, of the cell C_{ij}.

I *have not* demonstrated a way in which to find these two columns or two rows given the volume fraction information in the 3×3 block of cells B_{ij} centered on the cell C_{ij}. However, there are at least two algorithms currently in use that may provide the user with a way to choose the columns correctly, and hence produce a first-order accurate approximation to the slope of the curve $\mathbf{z}(s)$ in the center cell C_{ij}. These algorithms are the ones named LVIRA and ELVIRA in [23]. However this remains to be proven. Computational studies in [23] show that these algorithms are second-order accurate in the discrete max norm when the results are averaged over many (for example, one thousand) computations. However these algorithms may need to be modified in order to achieve strict second-order accuracy in the max norm without averaging.

In Theorem 24, I have proven that (126) holds provided that the maximum value

$$\kappa_{\max} = \max_s |\kappa(s)|$$

of the curvature $\kappa(s)$ of the interface $\mathbf{z}(s)$ in the 3×3 block of cells B_{ij} satisfies

$$\kappa_{\max} \leq C_\kappa \equiv \min\{C_h h^{-1}, (\sqrt{h})^{-1}\}, \tag{127}$$

where C_h is a constant that is independent of h. As $h \to 0$ the second constraint in (127) eventually becomes the condition that must be satisfied; that is, $(\sqrt{h})^{-1} < C_h h^{-1}$ for h small enough. It is natural to ask if this constraint is necessary, since I only need this constraint when the center column sum S_i is not exact; that is, I only use the constraint $\kappa_{\max} \leq (\sqrt{h})^{-1}$ to prove Theorem 15.

I have performed a number of computations in an effort to determine if the first constraint

$$\kappa_{\max} \leq C_h h^{-1}$$

is sufficient to ensure that (126) holds. These computations, together with several theorems I have proven in special cases when the center column sum S_i is not

exact,[12] lead me to believe that the second constraint in (127)

$$\kappa_{\max} \leq (\sqrt{h})^{-1}$$

is indeed necessary. However this issue requires further study.

In closing, I would like to emphasize that when the interface reconstruction algorithm is coupled to an adaptive mesh refinement algorithm, the parameter

$$H_{\max} = \min\{C_h (\kappa_{\max})^{-1}, (\kappa_{\max})^{-2}\}$$

can be used to develop a criterion for determining when to increase the resolution of the grid. Namely, the computation of the interface in a given cell C_{ij} is under-resolved whenever

$$h > H_{\max},$$

where $\kappa_{\max}$ is the maximum curvature of the interface over the 3×3 block of cells B_{ij} centered on C_{ij}, and hence the grid needs to be refined in a neighborhood of this block.

Acknowledgment

References

[1] I. Aleinov and E. G. Puckett, *Computing surface tension with high-order kernels*, Proceedings of the 6th International Symposium on Computational Fluid Dynamics (K. Oshima, ed.), American Society of Mechanical Engineers, 1995, pp. 6–13.

[2] J. U. Brackbill, D. B. Kothe, and C. Zemach, *A continuum method for modeling surface tension*, J. Comput. Phys. **100** (1992), no. 2, 335–354. MR 93c:76008 Zbl 0775.76110

[3] A. J. Chorin, *Flame advection and propagation algorithms*, J. Comput. Phys. **35** (1980), no. 1, 1–11. MR 81d:76061 Zbl 0425.76086

[4] _____, *Curvature and solidification*, J. Comput. Phys. **57** (1985), no. 3, 472–490. MR 86d: 80001 Zbl 0555.65085

[5] P. Colella, L. F. Henderson, and E. G. Puckett, *A numerical study of shock wave refraction at a gas interface*, Proceedings of the AIAA 9th Computational Fluid Dynamics Conference, 1989, pp. 426–439.

[6] J. J. Helmsen, P. Colella, E. G. Puckett, and M. R. Dorr, *Two new methods for simulating photolithography development in three dimensions*, Proceeedings of the 10th SPIE Optical/Laser Microlithography Conference, vol. 2726, SPIE, 1996, pp. 253–261.

---

[12]I have not included these theorems in this article.

[7] J. J. Helmsen, P. Colella, and E. G. Puckett, *Non-convex profile evolution in two dimensions using volume of fluids*, Technical report lbnl-40693, Lawrence Berkeley National Laboratory, 1997.

[8] L. F. Henderson, P. Colella, and E. G. Puckett, *On the refraction of shock waves at a slow-fast gas interface*, J. Fluid Mech. **224** (1991), 1–27.

[9] C. W. Hirt and B. D. Nichols, *Volume of fluid (VOF) method for the dynamics of free boundaries*, Journal of Computational Physics **39** (1981), 201–225.

[10] R. M. Hurst, *Numerical approximations to the curvature and normal of a smooth interface using high-order kernels*, MS thesis, University of California, Davis, 1995.

[11] D. R. Korzekwa, D. B. Kothe, K. L. Lam, E. G. Puckett, P. K. Tubesing, and M. W. Williams, *A second-order accurate, linearity-preserving volume tracking algorithm for free surface flows on 3-D unstructured meshes*, Proceedings of the 3rd ASME /JSME Joint Fluids Engineering Conference, American Society of Mechanical Engineers, 1999.

[12] D. B. Kothe, J. R. Baumgardner, S. T. Bennion, J. H. Cerutti, B. J. Daly, and K. S. Torrey, *Pagosa: A massively-parallel, multi-material hydro-dynamics model for three-dimensional high-speed flow and high-rate deformation*, technical report la-ur-92-4306, Los Alamos National Laboratory, 1992.

[13] D. B. Kothe, E. G. Puckett, and M. W. Williams, *Convergence and accuracy of kernel-based continuum surface tension models*, Fluid dynamics at interfaces (W. Shyy and R. Naranyan, eds.), Cambridge University Press, New York, 1999, pp. 347–356.

[14] D. B. Kothe, E. G. Puckett, and M. W. Williams, *Approximating interface topologies with applications to interface tracking algorithms*, Proceedings of the 37th AIAA Aerospace Sciences Meetings, American Institute of Aeronautics and Astronautics, 1999, pp. 1–9.

[15] P. Lax and B. Wendroff, *Systems of conservation laws*, Comm. Pure Appl. Math. **13** (1960), 217–237. MR 22 #11523 Zbl 0152.44802

[16] G. H. Miller and P. Colella, *A conservative three-dimensional Eulerian method for coupled solid-fluid shock capturing*, J. Comput. Phys. **183** (2002), no. 1, 26–82. MR 2003j:76080 Zbl 1057.76558

[17] G. H. Miller and E. G. Puckett, *Edge effects in molybdenum-encapsulated molten silicate shock wave targets*, J. Appl. Phys. **75** (1994), 1426–1434.

[18] ———, *A high-order godunov method for multiple condensed phases*, Journal of Computational Physics **128** (1996), 134–164.

[19] B. D. Nichols, C. W. Hirt, and R. S. Hotchkiss, *SOLA-VOF: A solution algorithm for transient fluid flow with multiple free boundaries*, technical report la-8355, Los Alamos National Laboratory, 1980.

[20] W. F. Noh and P. R. Woodward, *SLIC (Simple line interface calculation)*, technical teport ucrl-77651, Los Alamos National Laboratory, 1976.

[21] ———, *SLIC (Simple line interface calculation)*, Lecture Notes in Physics, no. 59, Springer, New York, 1976.

[22] J. E. Pilliod, *An analysis of piecewise linear interface reconstruction algorithms for volume-of-fluid methods*, MS thesis, University of California, Davis, 1992.

[23] J. E. Pilliod, Jr. and E. G. Puckett, *Second-order accurate volume-of-fluid algorithms for tracking material interfaces*, J. Comput. Phys. **199** (2004), no. 2, 465–502. MR 2005d:65145 Zbl 1126.76347

[24] S. Popinet and S. Zaleski, *A front-tracking algorithm for accurate representation of surface tension*, Int. J. Numer. Methods Fluids **30** (1999), 775–793. Zbl 0940.76047

[25] E. G. Puckett, *A volume-of-fluid interface tracking algorithm with applications to computing shock wave refraction*, Proceedings of the 4th International Symposium on Computational Fluid Dynamics (H. Dwyer, ed.), 1991, pp. 933–938.

[26] E. G. Puckett, L. F. Henderson, and P. Colella, *A general theory of anomalous refraction*, Shock Waves at Marseilles (R. Brun and L. Z. Dumitrescu, eds.), vol. 4, Springer, 1995, pp. 139–144.

[27] W. J. Rider and D. B. Kothe, *Reconstructing volume tracking*, J. Comput. Phys. **141** (1998), no. 2, 112–152. MR 99a:65200 Zbl 0933.76069

[28] R. Scardovelli and S. Zaleski, *Direct numerical simulation of free-surface and interfacial flow*, Annu. Rev. Fluid Mech. (1999), no. 31, 567–603. MR 99m:76002

[29] S. K. Stein and A. Barcellos, *Calculus and analytic geometry*, 5th ed., McGraw-Hill, 1992. Zbl 0375.26001

[30] M. Sussman, A. S. Almgren, J. B. Bell, P. Colella, L. H. Howell, and M. L. Welcome, *An adaptive level set approach for incompressible two-phase flows*, Proceedings of the 1996 ASME Fluids Engineering Summer Meeting (San Diego, CA), American Society of Mechanical Engineers, 1996, pp. 355–360.

[31] M. Sussman, A. S. Almgren, J. B. Bell, P. Colella, L. H. Howell, and M. L. Welcome, *An adaptive level set approach for incompressible two-phase flows*, J. Comput. Phys. **148** (1999), no. 1, 81–124. MR 99m:76098 Zbl 0930.76068

[32] M. Sussman and M. Ohta, *Improvements for calculating two-phase bubble and drop motion using an adaptive sharp interface method*, FDMP Fluid Dyn. Mater. Process. **3** (2007), no. 1, 21–36. MR 2008a:76117 Zbl 1153.76436

[33] M. Sussman and E. G. Puckett, *A coupled level set and volume-of-fluid method for computing 3D and axisymmetric incompressible two-phase flows*, J. Comput. Phys. **162** (2000), no. 2, 301–337. MR 2001c:76099 Zbl 0977.76071

[34] M. M. Sussman, *An adaptive mesh algorithm for free surface flows in general geometries*, Adaptive method of lines (A. V. Wouwer, P. Saucez, and W. E. Shiesser, eds.), Chapman & Hall/CRC, New York, 2001, pp. 207–213. MR 2002c:65004

[35] M. D. Torrey, L. D. Cloutman, R. C. Mjolsness, and C. W. Hirt, *NASA-VOF2D: A computer program for incompressible flows with free surfaces*, technical report LA-10612-MS, Los Alamos National Laboratory, December 1985.

[36] M. D. Torrey, R. C. Mjolsness, and L. R. Stein, *NASA-VOF3D: A three-dimensonal computer program for incompressible flows with free surfaces*, technical report LA-11009-MS, Los Alamos National Laboratory, 1987.

[37] M. W. Williams, *Numerical methods for tracking interfaces with surface tension in 3-D mold-filling processes*, Ph.D. thesis, University of California, Davis, 2000.

ELBRIDGE GERRY PUCKETT: egpuckett@ucdavis.edu
Department of Mathematics, University of California, Davis, CA 95616, United States

Communications in Applied Mathematics and Computational Science

pjm.math.berkeley.edu/camcos

See inside back cover or pjm.math.berkeley.edu/camcos for submission instructions.